TECHNISCHE UNIVERSITÄT
ILMENAU

PUCP

A contribution to the investigation of the rolling movement of mobile robots based on tensegrity structures

Thesis submitted by

B. Sc. – Ing. ENRIQUE ROBERTO CARRILLO LI

For the degree of

Master of Science in Mechanical Engineering

Supervising Professor

Pontificia Universidad Católica del Perú

Univ. Prof. Dr.-Ing. Jorge Antonio Rodríguez Hernández

Technische Universität Ilmenau

Prof. Dr.-Ing. habil Valter Böhm

Univ. Prof. Dr.-Ing. habil Klaus Zimmermann

Ilmenau, Germany
March – 2019

ERKLÄRUNG

Hiermit versichere ich, dass ich die vorliegende Masterarbeit selbstständig angefertigt und keine anderen als die angegeben Quellen und hilfsmittel verwendet habe.

Ilmenau, 20. März 2019

_____

Enrique Roberto Carrillo Li

KURZFÄSSUNG

Die vorliegende Arbeit hat ihren Ursprung in den Algorithmen und Ansätzen zur Analyse eines Roboters mit variabler Geometrie, der an der TU Ilmenau entwickelt wurde. Ein solcher Roboter hat einen anfangs zylindrischen Roboter in eine kegelstumpfförmige Geometrie umgewandelt, um um die vertikale Achse drehen zu können, die sich am Erzeugungspunkt eines solchen Kegels befindet. Die vorliegende Arbeit beginnt mit einer Einführung der Grundlagen für das Studium von Tensegrity-Strukturen; Später werden aus den variablen Parametern der geometrischen Beschreibung des Roboters die kinematischen Gleichungen von Position, Geschwindigkeit und Beschleunigung für jeden Punkt der Geometrie des Roboters ausgewertet. In demselben Kapitel wird eine Alternative zum Vorhersagen der Bahn des Roboters unter Verwendung einer Klothoide vorgeschlagen. Diese Kurve hat den Zweck, Gleichungen der Bewegungsbahn des geometrischen Mittelpunkts des Roboters zu geben. In einem folgenden Kapitel werden die Steuerungsalgorithmen für die Abrollbewegung des Roboters sowie eine mögliche konstruktive Form vorgestellt, die zuvor für eine ähnliche Anwendung verwendet wurde. Im letzten Kapitel werden verschiedene Alternative von Materialien für die Herstellung des Roboterkörpers sowie die Grundlagen eines Ansatzes zur Bewertung gekrümmter Zugstrukturen vorgestellt. Darüber hinaus wird eine Berechnungsform für die spätere Entwicklung der endgültigen Geometrie des Roboters vorgeschlagen.

ABSTRACT

The present work has its origin in the algorithms and approaches for the analysis of a robot of variable geometry developed in the TU Ilmenau. Such robot hat an initially cylindrical robot changes to a truncated conical geometry, in order to be able to rotate around the vertical axis located at the generating point of such a cone. The present thesis begins with a basic explanation of the foundations for the study of tensegrity structures; later, from the variable parameters of the geometric description of the robot, the kinematic equations of position, velocity and acceleration are evaluated for every point of the geometry of the robot. In the same chapter an alternative of predicting the path of the robot using a clothoid curve is proposed, this curve has the purpose of giving equations of the trajectory of the geometric center of the robot. In a following chapter, the control algorithms for the rolling movement of the robot are presented, as well as a possible constructive form previously used for a similar application. Finally, the last chapter presents alternative materials for manufacturing the body of the robot, as well as the bases of an approach for the evaluation of curved tensile structures; additionally, it proposes a form of calculation for later development of the final geometry of the robot.

RESUMEN

El presente trabajo tiene su origen en los algoritmos y planteamientos para el análisis de un robot rodante de geometría variable desarrollados en la TU Ilmenau. Tal robot inicialmente cilíndrico, cambia a una geometría cónica trunca, a fin de poder rotar alrededor del eje vertical situado en el punto generatriz de tal cono. La presente tesis inicia con una explicación básica de los fundamentos para el estudio de las estructuras tenségritas; posteriormente, a partir de los parámetros variables de la descripción geométrica del robot, se evalúan las ecuaciones cinemáticas de posición, velocidad y aceleración para todo punto del cono. En el mismo capítulo se propone una alternativa de predicción de la trayectoria del robot haciendo uso de una curva clotoide, tal curva tiene por finalidad dar ecuaciones de la trayectoria del centro geométrico del robot. En un siguiente capítulo, se presenta los algoritmos de control para el movimiento rodante del robot, así como una posible forma constructiva ya usada anteriormente para una aplicación similar. Finalmente, el último capítulo presente alternativas de materiales de fabricación del cuerpo del robot, así como las bases de un enfoque para la evaluación de estructuras tenségritas curvas; adicionalmente, propone una forma de cálculo para desarrollo posterior de la geometría final del robot.

TABLE OF CONTENTS

ACKNOWLEDGMENT

To my family, who has accompanied me and supported me during this large and difficult process. To them I dedicated this achievement

To Univ. Prof. Dr.-Ing. René Theska, without his priceless help, this achievement would have been impossible.

To the professors of the design area of the section of Mechanical Engineering of the PUCP, especially for Prof. Rodríguez, Prof. Barriga and Prof. Paulsen, who always have supported me, despite everything seemed lost.

To my thesis advisers at the TU Ilmenau, Univ. Prof. Dr.-Ing. habil Klaus Zimmermann and Prof. Dr.-Ing. habil Valter Böhm; for their support and their patience during the developing of this work and my studies.

To everyone, who has helped me during these difficult times, my endless gratitude.

LIST OF FIGURES

LISTA OF TABLES

LIST OF SYMBOLS

$\mathbf{A}$	Adjacency matrix
A	Coefficient of the Clothoid
${}^{0}\vec{a}_{sm}(t)$	Acceleration vector of each point of the spiral in system O_0 $\left[\mathrm{m/s^2}\right]$
${}^{F}\vec{a}_{sm}(t)$	Acceleration vector of each point of the spiral in system O_F $\left[\mathrm{m/s^2}\right]$
$\vec{a}_{0F}(t)$	Acceleration vector of the system O_0 respect the system O_F $\left[\mathrm{m/s^2}\right]$
$\mathbf{C}$	Connectivity matrix
$\mathbf{C}_B$	Connectivity matrix of bars
C_R	Conicity of the robot
$C_{R,\mathrm{f}}$	Final value of conicity in the segment
$C_{R,0}$	Initial value of conicity in the segment
$\mathbf{C}_S$	Connectivity matrix of strings
$\mathbf{C}_\theta^{\mathrm{T}}$	Connectivity matrix in cylindrical coordinates
$\mathbf{D}$	Equilibrium matrix
d_x	Displacement along X_F axis $\left[\mathrm{m}\right]$
d_y	Displacement along Y_F axis $\left[\mathrm{m}\right]$
d_z	Vertical displacement of the system O_0 $\left[\mathrm{m}\right]$

E_f	Elasticity modulus of the fiber material $\left[\mathrm{N/mm^2}\right]$
E_m	Elasticity modulus of the matrix material $\left[\mathrm{N/mm^2}\right]$
E_{rc}	Elasticity modulus on the radial direction of the composite material $\left[\mathrm{N/mm^2}\right]$
E_{tc}	Elasticity modulus on the tangential direction of the composite material $\left[\mathrm{N/mm^2}\right]$
Ed	Set of Edges
$\mathbf{F}_k$	Force matrix of a member
$\mathbf{F}$	Force matrix of the structure
${}^1F_{Wm}$	Force exerted by the m – mass in system O_1 $\left[\mathrm{N}\right]$
$\vec{f}_k$	Force field vector
$\vec{f}_n$	Vector of force
G	Set of degrees of each vertex
g	Gravity acceleration $\left[\mathrm{m/s^2}\right]$
In	Incidence matrix
$\mathbf{I}_G$	Tensor of mass moment of inertia respect center of gravity $\left[\mathrm{kg \cdot m^2}\right]$
k_m	Stiffness of the member
L	Element length matrix
L	Robot length $\left[\mathrm{m}\right]$
l_k	Actual length of the member

$l_{m,0}$	Rest length of the member
l_{Sm}	Polar longitudinal coordinate of a member
l_{Sn}	Polar longitudinal coordinate of a node
m_M	Vector of the m –th element
m_{lm}	Mass of the impulsive m – mass $[\mathrm{kg}]$
$\mathbf{M}$	Matrix of elements
$\mathbf{M}_\theta$	Matrix of elements expressed in cylindrical coordinates
$\mathbf{N}$	Matrix of nodes
$\mathbf{N}_\theta$	Matrix of nodes expressed in cylindrical coordinates
$\vec{N}(s)$	Normal vector of the clothoid
$\hat{n}(s)$	Unitary normal vector of the clothoid
$\hat{n}_0$	Unitary normal vector at the starting point
$\hat{n}_f$	Unitary normal vector at the final point
$\vec{n}$	Vector of nodes
$\hat{n}_I$	Unitary normal vector for inverted clothoid
n_N	Spatial coordinates of the n-th node
n_S	Number of spirals of the robot
$\mathbf{P}$	Matrix of external load on each node
$\mathbf{Q}$	Density force matrix
$\vec{q}$	Force density vector
$\mathbf{q}_{\mathrm{M}}$	Force density matrix version

R_K	Radius of curvature of the cone $[\mathrm{m}]$
R_{K0}	Starting value of curvature radius in the clothoid $[\mathrm{m}]$
R_{Kf}	Final value of curvature radius in the clothoid $[\mathrm{m}]$
${}^{F}\vec{R}_{sm}(t)$	Position vector of each point of the spiral in system O_F $[\mathrm{m}]$
r_0	Basic central radius $[\mathrm{m}]$
r_{0i}	Internal basis radius for the traveling spirals of the impulsive masses $[\mathrm{m}]$
r_{y+}	Radius located on y_1^+ in the robot $[\mathrm{m}]$
r_{y-}	Radius located on y_1^- in the robot $[\mathrm{m}]$
$\vec{r}_{0F}$	Position vector of the system O_0 respect the system O_F $[\mathrm{m}]$
${}^{1}\vec{r}_{Im}$	Position vector of the impulsive m – mass in system O_1 $[\mathrm{m}]$
${}^{1}\vec{r}_{sm}(t)$	Position vector of each point over the spirals in the system O_1 $[\mathrm{m}]$
${}^{F}r_{sm}(t)$	Position vector of each point of the spiral in system O_0 transformed into system O_F
${}^{0}\left[{}^{1}\dot{\vec{r}}_{sm}\right]$	Velocity of the points over the spirals in system O_1 transformed into system O_0 $[\mathrm{m/s}]$

$^{0}\left[{}^{1}\ddot{\vec{r}}_{sm} \right]$	Acceleration of the points over the spirals in system O_1 transformed into system O_0 $\left[\mathrm{m/s^2}\right]$
$^{0}\vec{r}_{sm}(t)$	Position vector of each point over the spirals in system O_0 $\left[\mathrm{m}\right]$
$^{1}\vec{r}_{Im}$	Position vector of the impulsive m – mass in system O_1 $\left[\mathrm{m}\right]$
$\vec{r}_{Im}$	Position vector of the impulsive m – mass over its spiral $\left[\mathrm{m}\right]$
r_{Sm}	Radial coordinate of a member
r_{Sn}	Radial coordinate of a node
$\vec{s}$	Internal force vector
s	Traveled distance over the curve $\left[\mathrm{m}\right]$
s_0	Starting value of traveling distance over the clothoid in the clothoid $\left[\mathrm{m}\right]$
s_f	Final value of traveling distance over the clothoid in the clothoid $\left[\mathrm{m}\right]$
$\vec{T}(s)$	Tangent vector of the clothoid
T_D	Torque to be reached by the system $\left[\mathrm{N}\cdot\mathrm{m}\right]$
$^{01}\mathbf{T}$	Transformation matrix from O_0 to O_1
$^{01}\mathbf{T}_x(t)$	Transformation matrix from O_0 to O_1 for turn around x_0
$^{01}\mathbf{T}_y(t)$	Transformation matrix from O_0 to O_1 for turn around y_0

${}^{F0}\mathbf{T}_Z(t)$	Transformation matrix turning around z_K
${}^{F0}\dot{\mathbf{T}}_Z(t)$	Derivate in the time of the transformation matrix from O_F to O_0
${}^{01}\dot{\mathbf{T}}(t)$	First derivate of the transformation matrix from O_0 to O_1
${}^{F1}\mathbf{T}(t)$	Transformation matrix from O_F to O_1
${}^{F1}\dot{\mathbf{T}}(t)$	Derivate in the time of the transformation matrix from O_F to O_1
${}^{1}\vec{T}$	Torque in system O_1 $[\mathrm{N}\cdot\mathrm{m}]$
${}^{1}T_y$	Torque exerted around y_1 $[\mathrm{N}\cdot\mathrm{m}]$
$\hat{t}_C$	Unitary tangent vector of the clothoid
$\hat{t}_{CI}$	Tangential normal vector for inverted clothoid
s_{x1}, s_{y1}, s_{z1}	Spiral shape equations.
$O_F X_F Y_F Z_F$	Inertial system of reference fix in the origin
$O_0 x_0 y_0 z_0$	Referential coordinate system of the robot
$O_1 x_1 y_1 z_1$	Basic system of coordinates for the robot
${}^{1}x_{\mathrm{Im}}, {}^{1}y_{\mathrm{Im}}, {}^{1}z_{\mathrm{Im}}$	Coordinates of the impulsive m – mass in system O_1 $[\mathrm{m}]$
$O_K x_K y_K z_K$	Coordinate system attached to the center of curvature
U	Coordinate difference matrix on the x axis
Ve	Set of vertex
V	Coordinate difference matrix on the y axis
V_m	Potential energy function of the member

V_f	Volume fraction of the fiber material over the total volume
V_m	Volume fraction of the matrix material over the total volume
${}^0\vec{v}_{sm}(t)$	Velocity vector of each point of the spiral in system O_0 $[\text{m/s}]$
${}^F\vec{v}_{sm}(t)$	Velocity vector of each point of the spiral in system O_F $[\text{m/s}]$
$\vec{v}_{0F}(t)$	Relative velocity vector of the system O_0 respect the system O_F $[\text{m/s}]$
$\vec{v}_{1\text{F}}(t)$	Relative velocity vector of the system O_1 respect the system O_F $[\text{m/s}]$
$\mathbf{W}$	Coordinate difference matrix on the z axis
${}^0x_{sm}, {}^0y_{sm}, {}^0z_{sm}$	Coordinates equations of the m – spiral referred to the system O_0
$\vec{x}_n$	Coordinate vector of the nodes on the x axis
$\vec{y}_n$	Coordinate vector of the nodes on the y axis
$\vec{z}_n$	Coordinate vector of the nodes on the z axis
${}^0\tilde{\boldsymbol{\alpha}}_{10}(t)$	Angular acceleration skew symmetric matrix of O_1 respect O_0 in system O_0 $\left[\text{rad/s}^2\right]$
${}^{\text{F}}\tilde{\boldsymbol{\alpha}}_{0\text{F}}(t)$	Angular acceleration skew symmetric matrix of O_0 respect O_F in system O_F $\left[\text{rad/s}^2\right]$
β_m	Position angle of the impulsive masses $[\text{rad}]$

β_{Pm}	Possible incremental value of β_m for the impulsive m – mass $[\text{rad}]$
Δs	Variation of the values of length of traveled curved inside the fitting clothoid $[\text{m}]$
$\Delta\theta$	Variation of the angle θ $[\text{rad}]$
$\Delta\xi$	Rotation angle for the clothoid
θ	Accumulated rotated angle $[\text{rad}]$
$\theta(t)$	**Pitch angle**, rotation around y_0 $[\text{rad}]$
θ_0	Starting value of θ in the clothoid $[\text{rad}]$
θ_f	Final value of θ in the clothoid $[\text{rad}]$
θ_{Sm}	Angular coordinate of a member
θ_{Sn}	Angular coordinate of a node
ϑ	Angular gap between spirals $[\text{rad}]$
Π	Total potential energy
Π_S	Strain Energy
Π_W	External work done by the external loads
χ	Conicity angle $[\text{rad}]$
χ_0	Starting value of conicity angle in the clothoid $[\text{rad}]$
χ_f	Final value of conicity angle in the clothoid $[\text{rad}]$
φ	Angle in the plane $x_0 - z_0$ respect the axis x_0 $[\text{rad}]$
$\phi(t)$	**Roll angle**, rotation around x_0 $[\text{rad}]$

$\dot{\phi}(t)$	Derivate in the time of the angle ϕ [rad/s]
Φ_m	Value of the angle turned by the impulsive mass [rad]
Φ_{mP}	Objective angle to reach by the impulsive masses [rad]
$\varphi_{\max}$	Developing angle of the spiral [rad]
φ_0	Initial rotate angle along y_1 axis [rad]
$\psi(t)$	**Yaw angle**, rotation around z_0 or parallel axis [rad]
$\dot{\psi}(t)$	Derivate in the time of the angle ψ [rad/s]
${}^0\tilde{\boldsymbol{\omega}}_{10}(t)$	Angular speed skew symmetric matrix of O_1 respect O_0 in system O_0 [rad/s]
${}^1\tilde{\boldsymbol{\omega}}_{10}(t)$	Angular speed skew symmetric matrix of O_1 respect O_0 in system O_1 [rad/s]
${}^F\tilde{\boldsymbol{\omega}}_{0F}(t)$	Angular speed skew symmetric matrix of O_0 respect O_F in system O_F [rad/s]
${}^F\tilde{\boldsymbol{\omega}}_{1F}(t)$	Angular speed skew symmetric matrix of O_1 respect O_F in system O_F [rad/s]
${}^0\vec{\omega}_{10}$	Angular velocity vector of O_1 respect O_0 in system O_0 [rad/s]

CHAPTER 1 BASIC CONCEPTS OF TENSEGRITY STRUCTURES

1.1 Introduction

Is a fact that we almost nothing have discovered, we just have found our knowledge in the nature, the tensegrity structures are not an exception; we can have turn our sight wherever to find such structures even inside our bodies.

Tensegrity is a word coined by Richard Buckminster Fuller as the joint of the words 'tensional' and 'integrity', which makes referent to the integrity of a stable structured in equilibrium by continuous structural member in tension and discontinuous structural members in compression. Such structures are present in many topics of the nature; some of them are, even, inside of us such our shoulder joints or the structures of our legs. The nature has developed this knowledge in its path to its continuous improvement, called by us as evolution; we take advantage of this technology for our purposes in fields as Art, Beauty, Architecture and Engineering.

This kind of structures offers to the engineering field the possibility to develop machines which can support highest load with a light structure, also the possibility to change the geometry of a machine to perform different task according our convenience. In this field, this work is a contribution to developing of rolling robot based on these structures. Some further application for this kind of robot or mechanism could be a new technology for the direction control of vehicles or robots in general.

The fundamentals principles for the calculus of this kind of structures are presented in the first chapter, all those concepts can be found in different books specialized on this

study field, but this is a recompilation of some concepts, even from the graph theory used as a mathematical basis for the description of this structures in lineal cases.

The main contribution is the developing of the kinematic of the robot, which is subjected to rotations along three different axis and internal geometrical changes which add a complexity to the final expression, a new approach for the prediction of the trajectory, taking advantages of the variation of the curvature radius, is presented; this prediction procedure uses the equation of a curved known as clothoid.

Not less important is the control algorithm used for the rolling movements; some ideas for the developing of a control system are presented.

Finally, owing to the large deformation which must be exerted to the robot, the material selection for the body of the robot has an important role, due to depending on its mechanical behavior we can obtain different effects for certain direction over we apply the force which makes the geometrical transformation of the robot.

This work is a step for the final developing of this kind of machines, a large amount of additional work is required to arrive to a final design.

Figure 1-1 Tensegrity structure model of a human knee. Source: [Pinterest]

About the last one, these structures take a big advantage due their low force density and their multiple equilibrium configurations that allow them to achieve multiple tasks; also those structures can be controlled by sensors and actuators.

In this chapter, the basic definitions about tensegrity structures, static and stability analysis will be briefly treaded.

1.2 Definitions

The following definitions are terms which are going to be used in the following sections of this chapter.

- **Bodies**: these are elements, which are only subjected to compression forces or bending moments. These elements can be modeled as discontinuous rigid or deformable bodies depending on the desirable movement to achieve.
- **String**: These elements only support traction forces. These components are continuous and flexible. Sometimes, these elements are modeled as springs which can be subjected to compression forces, but by definition, they are considered only as traction members.
- **Configuration and connectivity:** The positions and orientation of all rigid bodies is called configuration and the connections between rigid bodies by strings are called as connectivity.
- **Stability:** It is a condition, in which, there is not relative displacement between the members of a structure by action of its inner forces.
- **Tensegrity configuration:** It is a configuration of bodies for which exists string connectivity able to stabilize the configuration in absence of external forces.
- **Tensegrity system:** It is composed of a set of string connected to a tensegrity configuration. Also, it must be prestressable in absence of external forces.
- **Class of tensegrity system:** It a way to classify tensegrity systems. To know which class is a system there is only a simple rule: “The class number is equal to the maximum number of bodies in contact on at a node. The main reason for this

definition is when there are not bodies in contact, system class 1, these only works axially; otherwise there is bending loads. The mathematical treatment when bending is present is much complex as when there are only axial forces.

- **Stable equilibrium:** A Tensegrity system is a stable equilibrium, if the structure returns to the original given configuration after the application of arbitrarily small perturbations anywhere within the configuration.

1.2.1 Fundamentals of Tensegrity Structures

On basis of the definition of tensegrity system we can define the following fundamental tensegrity structure. On the first level, the simplest tensegrity is a single body and a string [a) Figure 1-2]; additionally, the simplest nontrivial tensegrity structure is composed of two bars and four strings [b) Figure 1-2].

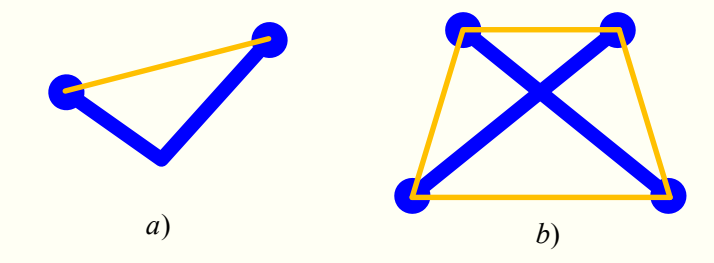

Figure 1-2 Fundamental tensegrity structures

Finally these structures are projected in three dimensions, so they are called as tensegrity prism.

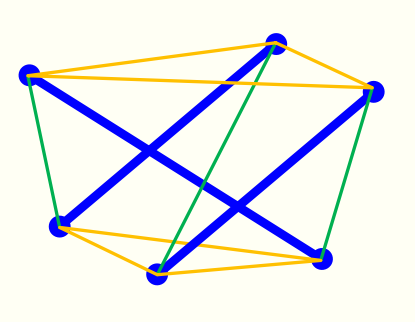

Figure 1-3 Basic tensegrity prism

1.3 Static Analysis

This analysis begins with developing mathematical algorithms to model stable equilibrium, stiffness properties, mass and the relationships between force and configuration of tensegrity systems. To begin, we have to define the geometry structure mathematically, which translated to tensegrity language, means describe nodes, members and the connectivity as a vectors and matrixes. Most cases the members are considered or assumed as straight, therefore the structure can be modeled using Graph theory as directed graph.

1.3.1 Fundamentals of Graph Theory

A graph is composed of vertices and edges. It can represent many real situations as an electric circuit or a road map, etc. An example is showed in the following figure:

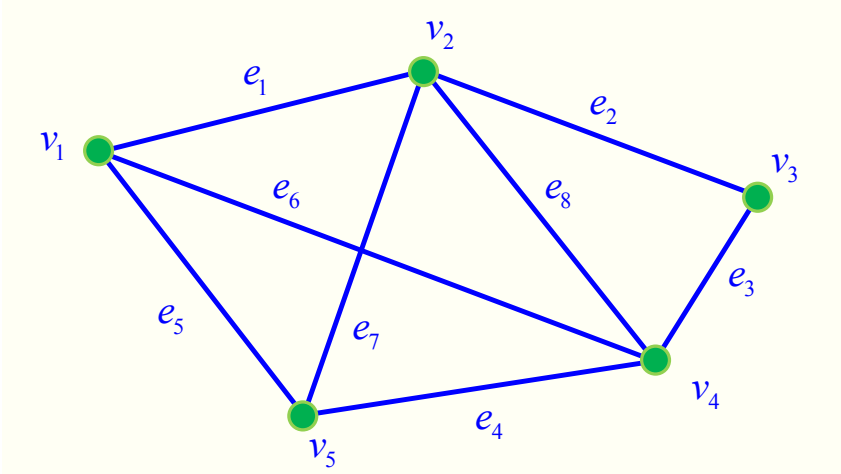

Figure 1-4 Graph structure

Let Ve be a set containing all the coordinates of the nodes and Ed be a set containing the pairs of nodes whose compose an edge. According with this definition and the example depicted at the previous figure, we have:

$$\mathrm{Ve} = \{v_1 \quad v_2 \quad v_3 \quad v_4 \quad v_5\}$$

$$\mathrm{Ed} = \{(v_1 \quad v_2) \quad (v_2 \quad v_3) \quad (v_3 \quad v_4) \quad (v_4 \quad v_5) \quad (v_1 \quad v_5) \quad (v_1 \quad v_4) \quad (v_2 \quad v_5) \quad (v_2 \quad v_4)\}$$

Where

Ve	Set of vertex
Ed	Set of Edges

Also a Graph can have a curved edges or unconnected nodes. It is also necessary add the concept of vertex degree which defined by the number of edges which are connected at the vertex. Additionally with this definition, we have the set G as function of Ve and Ed, this set contains the degree of all the vertex of the graph. From the previous example:

$$G = (\mathrm{Ve}, \mathrm{Ed}) = \{3 \quad 4 \quad 2 \quad 4 \quad 3\}$$

Where

G	Set of degrees of each vertex

Additionally we define $\delta(G)$ as the minimum degree and $\Delta(G)$ as the maximum degree of the vertex respectively. Finally, walks are defined as the way of getting from one vertex to another; it is a sequence of edges.

Another kind of graphs is the so-called directed graph which is used in tensegrity structures. These graphs have a sense of connection such that there is an initial vertex and a final vertex.

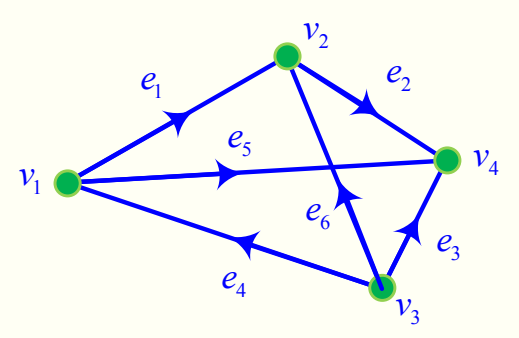

Figure 1-5 Directed graph

The application of this theory on tensegrity structures is the matrix representation of the directed graph. We define the adjacency matrix and the incidence matrix to achieve it.

The adjacency matrix can be defined as a matrix $n \times n$ where n is the number of vertices of the graph $G = (\mathrm{Ve}, \mathrm{Ed})$; each $ij-\text{th}$ entry is the number of edges connecting the vertex i and vertex j; additionally, this matrix is symmetric $A = A^T$. From the example of the Figure 1-4, its adjacency matrix is defined as follow:

$$\mathbf{A} = \begin{bmatrix} 0 & 1 & 0 & 1 & 1 \\ 1 & 0 & 1 & 1 & 1 \\ 0 & 1 & 0 & 1 & 0 \\ 1 & 1 & 1 & 0 & 1 \\ 1 & 1 & 0 & 1 & 0 \end{bmatrix}$$

Where

$\mathbf{A}$ Adjacency matrix

For directed matrix, the $ij-\text{th}$ entry is the number of edges which come out of vertex i and go into vertex j. The adjacency matrix of the Figure 1-5 is as follow:

$$\mathbf{A} = \begin{bmatrix} 0 & 1 & 0 & 1 \\ 0 & 0 & 0 & 1 \\ 1 & 1 & 0 & 1 \\ 0 & 0 & 0 & 0 \end{bmatrix}$$

The other matrix which can represent a graph is the incidence matrix, it can be defined as a matrix $n \times m$ where n is the number of vertices and m is the number of edges. For a non – directed graph each $ij-\text{th}$ entry is determinated through the following rule:

$$a_{ij} = \begin{cases} 1 & \text{if } v_i \text{ is an end vertex of } e_j \\ 0 & \text{otherwise} \end{cases} \tag{1.1}$$

From the example of the Figure 1-4, its incidence matrix is defined as follow:

$$\mathbf{In} = \begin{bmatrix} 1 & 0 & 0 & 0 & 1 & 1 & 0 & 0 \\ 1 & 1 & 0 & 0 & 0 & 0 & 1 & 1 \\ 0 & 1 & 1 & 0 & 0 & 0 & 0 & 0 \\ 0 & 0 & 1 & 1 & 0 & 1 & 0 & 1 \\ 0 & 0 & 0 & 1 & 1 & 0 & 1 & 0 \end{bmatrix}$$

Where

In Incidence matrix

For directed graph, the incidence matrix which in which is based the connectivity matrix of tensegrity structures is defined by the following rules:

$$a_{ij} = \begin{cases} 1 & \text{if } v_i \text{ is the initial vertex of } e_j \\ -1 & \text{if } v_i \text{ is an terminal vertex of } e_j \\ 0 & \text{otherwise} \end{cases} \tag{1.2}$$

The incidence matrix of the Figure 1-5 is as follow:

$$\mathbf{In} = \begin{bmatrix} 1 & 0 & 0 & -1 & 1 & 0 \\ -1 & 1 & 0 & 0 & 0 & -1 \\ 0 & 0 & 1 & 1 & 0 & 1 \\ 0 & -1 & -1 & 0 & -1 & 0 \end{bmatrix}$$

1.3.2 Geometry Description

Once the incidence matrix for a directed graph is defined, we can deal with this concept, in order to build a set of matrix which can describe more precisely the position and orientation of the elements of the structure.

To explain this idea, we take the following example – structure taken from [2]:

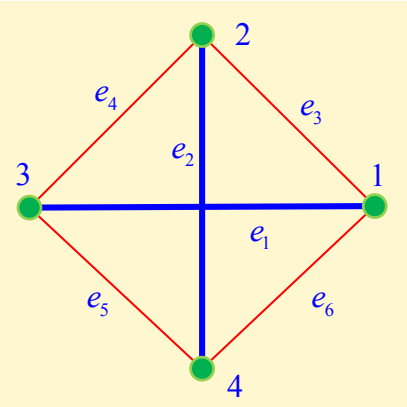

Figure 1-6 Example Structure. Source: [2]

Again, in this introduction, we only deal with linear elements, that means, we do not work with curved element. This treatment for curved tensegrity will be introduced in further chapters.

The first element highlighted is the node; this element defines the spatial position and length of the members of the structure. Each node has a position on the space which is defined by its Cartesian coordinates. If we gather all the nodes and build a matrix with their coordinates, we can define the matrix of nodes:

$$n_N = \begin{bmatrix} x_N & y_N & z_N \end{bmatrix}^T$$

$$\mathbf{N} = \begin{bmatrix} n_1 & n_2 & \cdots & n_N \end{bmatrix}$$

Where

n_N	Spatial coordinates of the n – th node
$\mathbf{N}$	Matrix of nodes

In the same way, we can define a matrix of elements, each of them are defined by a pair of nodes.

$$\vec{m}_M = \begin{bmatrix} x_M & y_M & z_M \end{bmatrix}^T$$

$$\mathbf{M} = \begin{bmatrix} \vec{m}_1 & \vec{m}_2 & \cdots & \vec{m}_M \end{bmatrix}$$

Where

m_M	Vector of the m –th element
$\mathbf{M}$	Matrix of elements

The relationship between those matrixes is the connectivity matrix; such matrix defines which node connects with what node, in order to establish the complete structure.

The incidence matrix, assuming a directed graph to replace the structure, is related with the connectivity matrix by the following mathematical expression:

$$\mathbf{C}^T = \mathbf{In} \tag{1.3}$$

Where:

$\mathbf{C}$ Connectivity matrix

This matrix, as the incidence matrix, is only made of ones, zeros and minus ones.

Then, we can set the relationship between nodes and member:

$$\mathbf{M} = \mathbf{N}\mathbf{C}^T \tag{1.4}$$

From the example of the Figure 1-6, we have the following node matrix:

$$\mathbf{N} = \begin{bmatrix} 1 & 0 & -1 & 0 \\ 0 & 1 & 0 & -1 \end{bmatrix}$$

Then, we set the connectivity matrix, distinguish between bar elements and string elements, such matrix is the transpose of the incidence matrix:

$$\mathbf{C} = \begin{bmatrix} \mathbf{C}_B \\ \mathbf{C}_S \end{bmatrix} = \begin{bmatrix} -1 & 0 & 1 & 0 \\ 0 & -1 & 0 & 1 \\ -1 & 1 & 0 & 0 \\ 0 & -1 & 1 & 0 \\ 0 & 0 & -1 & 1 \\ 1 & 0 & 0 & -1 \end{bmatrix} = \begin{bmatrix} \vec{c}_1 \\ \vec{c}_2 \\ \vec{c}_3 \\ \vec{c}_4 \\ \vec{c}_5 \\ \vec{c}_6 \end{bmatrix}$$

Where:

$\mathbf{C}_B$ Connectivity matrix of bars

$\mathbf{C}_S$ Connectivity matrix of strings

Using the expression (1.4):

$$\mathbf{M} = \begin{bmatrix} 1 & 0 & -1 & 0 \\ 0 & 1 & 0 & -1 \end{bmatrix} \begin{bmatrix} -1 & 0 & -1 & 0 & 0 & 1 \\ 0 & -1 & 1 & -1 & 0 & 0 \\ 1 & 0 & 0 & 1 & -1 & 0 \\ 0 & 1 & 0 & 0 & 1 & -1 \end{bmatrix}$$

$$\mathbf{M} = \begin{bmatrix} -2 & 0 & -1 & -1 & 1 & 1 \\ 0 & -2 & 1 & -1 & -1 & 1 \end{bmatrix}$$

1.3.3 Equilibrium Matrix

From this section, we begin to work with coordinate differences using the following notation:

$$u_k = x_i - x_j \tag{1.5}$$

$$v_k = y_i - y_j \tag{1.6}$$

$$w_k = z_i - z_j \tag{1.7}$$

The coordinate difference vector in each direction is given by the connectivity matrix as follow:

$$\vec{u} = \mathbf{C}\vec{x}_n \tag{1.8}$$

$$\vec{v} = \mathbf{C}\vec{y}_n \tag{1.9}$$

$$\vec{w} = \mathbf{C}\vec{z}_n \tag{1.10}$$

Where

$\vec{x}_n$ Coordinate vector of the nodes on the x axis

$\vec{y}_n$ Coordinate vector of the nodes on the y axis

$\vec{z}_n$ Coordinate vector of the nodes on the z axis

They can be expressed as matrix using a diagonal matrix for each of them:

$$\mathbf{U} = \text{diag}\left(\vec{u}\right) \tag{1.11}$$

$$\mathbf{V} = \text{diag}\left(\vec{v}\right) \tag{1.12}$$

$$\mathbf{W} = \text{diag}\left(\vec{w}\right) \tag{1.13}$$

Where

U Coordinate difference matrix on the x axis

V Coordinate difference matrix on the y axis

W Coordinate difference matrix on the z axis

In terms of matrix, we can get the length matrix using the following operation:

$$\mathbf{L}^2 = \mathbf{U}^2 + \mathbf{V}^2 + \mathbf{W}^2 \tag{1.14}$$

Where

L Element length matrix

We can express the element matrix as a composition of the difference vectors:

$$\mathbf{M} = \begin{bmatrix} \vec{u} \\ \vec{v} \\ \vec{w} \end{bmatrix} \tag{1.15}$$

In order to determine de equilibrium within the structure, we have isolated the node 1 from the Figure 1-6.

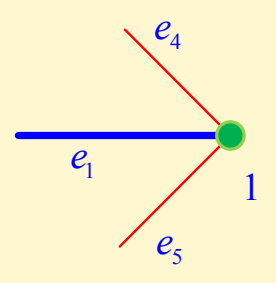

Figure 1-7 Node Analysis

On each member of the structure, there is an internal force due to the prestress. Since the nature of the elements; for example, the element 4 and 5 are strings; this element only can support tensile forces. Additionally, for optimization reasons, the element 1, which is a bar, only can carry compression forces.

The internal forces within the elements are going to be assigned in a vector:

$$\vec{s} = \begin{bmatrix} -s_1 & -s_2 & s_3 & s_4 & s_5 & s_6 \end{bmatrix}$$

The forces of the element 1 and 2 have an opposite sign, because those elements are bars; it means that the forces along the bars are compressive.

Where

$\vec{s}$ Internal force vector

From the Figure 1-7:

$$\mathbf{U} = \begin{bmatrix} -2 & 0 & 0 & 0 & 0 & 0 \\ 0 & 0 & 0 & 0 & 0 & 0 \\ 0 & 0 & -1 & 0 & 0 & 0 \\ 0 & 0 & 0 & -1 & 0 & 0 \\ 0 & 0 & 0 & 0 & 1 & 0 \\ 0 & 0 & 0 & 0 & 0 & 1 \end{bmatrix} \qquad \mathbf{V} = \begin{bmatrix} 0 & 0 & 0 & 0 & 0 & 0 \\ 0 & -2 & 0 & 0 & 0 & 0 \\ 0 & 0 & 1 & 0 & 0 & 0 \\ 0 & 0 & 0 & -1 & 0 & 0 \\ 0 & 0 & 0 & 0 & -1 & 0 \\ 0 & 0 & 0 & 0 & 0 & 1 \end{bmatrix}$$

A systematic decomposition over each axis can be made using the geometrical relation of the elements; for example, in the element 1 for the analysis on the node 1:

$$s_1 \frac{x_2 - x_1}{l_1} \times C_{(1,1)} \tag{1.16}$$

Where:

l_k Actual length of the member

For all the elements connected to the node 1, it can be simplified using the following product:

$$\mathbf{C}_{(:,1)}^{\mathrm{T}} \mathbf{U} \mathbf{L}^{-1} \vec{s}^{\,T} = 0 \tag{1.17}$$

For the example, the internal forces over the axis x in the node 1 have the following equilibrium equation:

$$\begin{bmatrix} s_1 & 0 & -\frac{s_3}{\sqrt{2}} & 0 & 0 & -\frac{s_6}{\sqrt{2}} \end{bmatrix}$$

$$-s_1 + \frac{s_3}{\sqrt{2}} + \frac{s_6}{\sqrt{2}} = 0$$

And over axis y

$$-\frac{s_3}{\sqrt{2}} + \frac{s_6}{\sqrt{2}} = 0$$

This result can be proven making the free body diagram of the node 1:

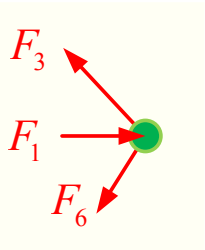

Figure 1-8 Free body diagram of a node

Overall the structure, the matrix product over each axis:

$$\mathbf{D}_x = \mathbf{C}^{\mathrm{T}}\mathbf{U}\mathbf{L}^{-1} \tag{1.18}$$

$$\mathbf{D}_y = \mathbf{C}^{\mathrm{T}}\mathbf{V}\mathbf{L}^{-1} \tag{1.19}$$

Finally we can express de equilibrium matrix as composition of $\mathbf{D}_x$ and $\mathbf{D}_y$

$$\mathbf{D} = \begin{bmatrix} \mathbf{D}_x \\ \mathbf{D}_y \end{bmatrix}$$

Expressing as a matricial equation:

$$\mathbf{D}\begin{bmatrix} \vec{s}^{\,\mathrm{T}} \\ \vec{s}^{\,\mathrm{T}} \end{bmatrix} = 0 \tag{1.20}$$

Where

$\mathbf{D}$ Equilibrium matrix

1.3.4 Force Density Matrix

The force density of a member can be expressed as the liner density of force along the element:

$$q_k = \frac{s_k}{l_k} \tag{1.21}$$

Also, we can define a force density vector, which gather the density in all the elements.

$$\vec{q} = \mathbf{L}^{-1}\,\vec{s} \tag{1.22}$$

As the previous vectors, the force density vector can be expressed as a diagonal matrix:

$$\mathbf{q}_{\mathrm{M}} = \begin{bmatrix} q_1 & 0 & 0 & 0 & 0 & 0 \\ 0 & q_2 & 0 & 0 & 0 & 0 \\ 0 & 0 & q_3 & 0 & 0 & 0 \\ 0 & 0 & 0 & q_4 & 0 & 0 \\ 0 & 0 & 0 & 0 & q_5 & 0 \\ 0 & 0 & 0 & 0 & 0 & q_6 \end{bmatrix}$$

Where

$\vec{q}$ Force density vector

$\mathbf{q}_{\mathrm{M}}$ Force density matrix version

From the equilibrium equation (1.20), we can rewrite the equation using density forces; For example, along the x axis:

$$\mathbf{D}_x\vec{s} = \mathbf{C}^{\mathrm{T}}\mathbf{U}\mathbf{L}^{-1}s = \mathbf{C}^{\mathrm{T}}\mathbf{U}\vec{q}$$

$$\mathbf{D}_x\vec{s} = \mathbf{C}^{\mathrm{T}}\mathbf{q}_{\mathrm{M}}\,\vec{u}$$

$$\mathbf{D}_x\vec{s} = \mathbf{C}^{\mathrm{T}}\mathbf{q}_{\mathrm{M}}\mathbf{C}\,\vec{x}_n \tag{1.23}$$

The matricial product in the equation (1.23):

$$\mathbf{Q} = \mathbf{C}^{\mathrm{T}}\mathbf{q}_{\mathrm{M}}\mathbf{C} \tag{1.24}$$

The result of this product is called density force matrix. For the example of the Figure 1-7:

$$\mathbf{Q} = \begin{bmatrix} q_1+q_3+q_6 & -q_3 & -q_1 & -q_6 \\ -q_3 & q_2+q_3+q_4 & -q_4 & -q_2 \\ -q_1 & -q_4 & q_1+q_4+q_5 & -q_5 \\ -q_6 & -q_2 & -q_5 & q_2+q_5+q_6 \end{bmatrix}$$

Where:

$\mathbf{Q}$ Density force matrix

Therefore, we can simplify the equilibrium equation as follow:

$$\mathbf{Q}\vec{x}_n = 0 \tag{1.25}$$

$$\mathbf{Q}\vec{y}_n = 0 \tag{1.26}$$

Although these expressions can be used, also, for fixed structure as well free standing structures, there is a different treatment for each of them; in this particular case, we are dealing with free standing structures, which do not have fixed nodes.

1.4 Stability

In this section, the principles of potential energy and stability will be treated. These concepts are fundamental, in order to find a self – standing structure which can be stable under prestress conditions.

A tensegrity structure is subjected to large deformation, due its flexibility. Finally, the energy functions are going to be applied in the further dynamic analysis.

1.4.1 Relation between Potential and Force

The entire structural member are subjected to internal force due the prestress, each of this member has an internal energy, which is able to be described by the coming relation:

$$V_m = \frac{1}{2} k_m \left(l_m - l_{m,0} \right)^2 = F\left(l_m \right) \tag{1.27}$$

Where:

$l_{m,0}$ Rest length of the member

k_m Stiffness of the member

V_m Potential energy function of the member

Energy is a function of the length of the member and, also, this function is called potential function. If we derivate this function on each direction of the coordinate system in which we defined our structure, we can find the force at each node.

$$\vec{f}_k = -\nabla V = \begin{pmatrix} -f_x & -f_y & -f_z \end{pmatrix} \tag{1.28}$$

Where:

$\vec{f}_k$ Force Field vector

Taking the partial derivate over the x axis and applying the chain rule:

$$f_x = -\frac{dV(l_k)}{dl_k}\frac{l_k}{dx}$$

In all directions, we obtain:

$$\vec{f}_k = -\begin{pmatrix} \frac{dV(l)}{dl}\frac{dl}{dx} & \frac{dV(l)}{dl}\frac{dl}{dy} & \frac{dV(l)}{dl}\frac{dl}{dz} \end{pmatrix}$$

Factorizing and simplifying:

$$\vec{f}_k = -\frac{V_k'(l)}{l_k}\begin{pmatrix} x_k & y_k & z_k \end{pmatrix} \tag{1.29}$$

The derivate of the potential energy of a member respect of its length is the force result of the prestress of the structure.

$$s_k = \frac{dV(l)}{dl} = V'(l) = k_m\left(l_m - l_{m,0}\right) \tag{1.30}$$

Replacing (1.21) and (1.30) in (1.29):

$$\vec{f}_k = -q_k\vec{m}_k \tag{1.31}$$

In order to know, the action of this force in the nodes, it necessary to make a mathematical arrangement:

$$\vec{f}_{nk} = q_k\left(c_k^{\mathrm{T}} \otimes \vec{m}_k\right) \tag{1.32}$$

Where:

$\vec{f}_n$ Vector of forces

This operation is called Kronecker product and also is denoted by the symbol $\otimes$. This operation gives a column matrix which is the vectored form of the following expression:

$$\mathbf{F}_k = -q_k \left(\vec{m}_k \times \vec{c}_1 \right) \tag{1.33}$$

Over all the nodes, considering that action of the force in the nodes where the element is connected, we obtain

$$\mathbf{F} = \mathbf{M}\mathbf{q}_{\mathrm{M}}\mathbf{C} \tag{1.34}$$

Where:

$\mathbf{F}_k$ Force matrix of a member

$\mathbf{F}$ Force matrix of the structure

In equilibrium

$$\mathbf{M}\mathbf{q}_{\mathrm{M}}\mathbf{C} = \mathbf{0} \tag{1.35}$$

1.4.2 Potential Energy

In a hypothetical case, we add an infinitesimal displacement as a result of the external load applied over the structure, we can define two kinds of energy which vary due this displacement.

For any instant of time, the total amount of potential energy along all the structure is defined by:

$$\Pi = \Pi_S - \Pi_W$$

Where:

Π Total potential energy

Π_S Strain Energy

Π_W External work done by the external loads

Mathematically, we can define the strain Energy in the structure as the sum of all the energy stored in all the member of the structures:

$$\Pi_S = \sum_{k=1}^{m} V_k\left(l_k\right) \tag{1.36}$$

We can express the potential energy as a function of the nodes. So this can be intended as the coordinates of the nodes define the member, which have lengths, those define the potential energy inside each of them.

The external work done by the external loads, it is useful to deal with the following mathematical arrangement:

$$\vec{n} = \mathrm{vec}\left(\mathbf{N}\right) \tag{1.37}$$

Where:

$\vec{n}$ Vector of nodes

The displacement of the nodes means the variations of the coordinates of them. Due the loads are assumed applied in the nodes, the work on each direction can be calculated using the following equation:

$$\Pi_W = \mathrm{vec}\left(\mathbf{P}\right)^{\mathrm{T}} \times \mathrm{vec}\left(\Delta\mathbf{N}\right) \tag{1.38}$$

Where:

$\mathbf{P}$ Matrix of external load on each node

1.4.3 Stiffness Matrix

All the potential energy in the structure can be defined as a function of the nodes and if we add an infinitesimal displacement of the nodes, in consequence, the total energy will vary. This can be approximated by Taylor Series as follow:

$$\Pi\left(n+\delta n\right) = \Pi\left(n\right) + \left(n-\delta n\right)\left(\mathbf{F}\left(n\right) + \mathrm{vec}\left(\mathbf{P}\right)\right) + \frac{\left(n-\delta n\right)^2}{2}\mathbf{K}\left(n\right) + O_3\left(n-\delta n\right) \tag{1.39}$$

If the last expression is showed in term of the differential and truncate the expression in the third term:

$$\Delta\Pi = \left(\mathbf{F}(n) + \mathrm{vec}(\mathbf{P})\right)(\Delta n) + \frac{(\Delta n)^2}{2}\mathbf{K}(n) \tag{1.40}$$

Where:

K Stiffness Matrix

The Stiffness matrix can be intended as the second derivative of the potential function as follow:

$$\mathbf{K}(n) = -\nabla \cdot \left(-\nabla \cdot V(n)\right)$$

Or

$$\mathbf{K}(n) = -\partial_n \left(-\partial_n V(n)\right) \tag{1.41}$$

In the same way

$$\vec{f}_{k,n}(n) = c_k^{\mathrm{T}} \otimes \partial_n V_k(n) \tag{1.42}$$

Also

$$\vec{f}_{n,k} = \mathrm{vec}(\mathbf{F}_k) \tag{1.43}$$

If we only derivate the force field produced by the potential energy of each element:

$$\partial_n \vec{f}_k = \partial_n \left(-\frac{V_k'(l_k)}{l_k}\vec{m}_k\right) \tag{1.44}$$

Applying the chain rule:

$$\partial_n \vec{f}_k = \left(\frac{V_k'(l_k)}{l_k}\partial_n \vec{m}_k\right) + \partial_n \left(\frac{V_k'(l_k)}{l_k}\right)\vec{m}_k$$

$$\partial_n \vec{f}_k = \mathbf{I}_n\, q_k + \left(\frac{\partial_n V_k'(l_k) - V_k'(l_k)\partial_n l_k}{l_k^2}\right)\vec{m}_k$$

$$\partial_n \vec{f}_k = \mathbf{I}_n\, q_k + \left(V_k''(l_k)\vec{m} - V_k'(l_k)\frac{\vec{m}}{l_k}\right)\frac{\vec{m}_k}{l_k^2}$$

$$L_k = -\partial_n \vec{f}_k = \mathbf{I}_n\, q_k + \left(k_k - q_k\right)\frac{\vec{m}_k \vec{m}_k^{\mathrm{T}}}{l_k^2} \tag{1.45}$$

The expression (1.45) is a matrix, which is the singular stiffness of each element.The connection between nodes is made using the following mathematical arrangement:

$$\mathbf{K}_k = c_k^{\mathrm{T}} c_k \otimes L_k \tag{1.46}$$

This can be watched in the following figure:

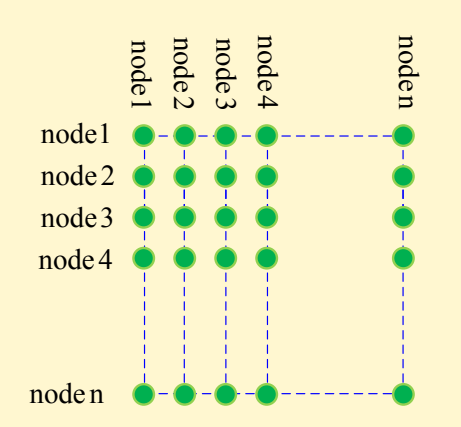

Figure 1-9 Arrangement of the Stiffness matrix

According with [2], we can deal the expression (1.46) as follow:

$$\mathbf{K}(n) = \left(\mathbf{C}^{\mathrm{T}} \otimes \mathbf{I}_3\right)\mathbf{I}_{\mathrm{M}}\left(\mathbf{C} \otimes \mathbf{I}_3\right) \tag{1.47}$$

Where:

$$\mathbf{I}_{\mathrm{M}} = \mathrm{diag}\left[\mathbf{L}_1, \mathrm{K}\ , \mathbf{L}_m\right]$$

Also the equation can be separated in two terms:

$$\mathbf{K}(n) = \mathbf{K}_q(n) + \mathbf{K}_\phi(n) \tag{1.48}$$

Where:

$$\mathbf{K}_q = \mathbf{C}^{\mathrm{T}} \mathbf{q}_{\mathrm{M}} \mathbf{C} \otimes \mathbf{I}_n \tag{1.49}$$

$$\mathbf{K}_\phi = \left(\mathbf{C}^{\mathrm{T}} \otimes \mathbf{I}_3\right)\mathbf{\Phi}\left(\mathbf{C} \otimes \mathbf{I}_3\right) \tag{1.50}$$

$$\mathbf{\Phi} = \text{diag}\left[\left(k_1 - q_1\right)\frac{\mathbf{r}_1\mathbf{r}_1^{\mathrm{T}}}{l_1^2}, \mathrm{K}\ , \left(k_m - q_m\right)\frac{\mathbf{r}_m\mathbf{r}_m^{\mathrm{T}}}{l_m^2} \right] \tag{1.51}$$

The component $\mathbf{K}_q$ is related to the prestress which the structure is subjected and the second component $\mathbf{K}_\phi$ is referred from the material.

For the example of the Figure 1-6, we have the following stiffness matrix:

$$\mathbf{L}_1 = \begin{bmatrix} k_B & 0 \\ 0 & -q_1 \end{bmatrix} \qquad \mathbf{L}_2 = \begin{bmatrix} -q_2 & 0 \\ 0 & k_b \end{bmatrix} \qquad \mathbf{L}_3 = \frac{1}{2}\begin{bmatrix} k_s + q_3 & -\left(k_s - q_3\right) \\ -\left(k_s - q_3\right) & k_s + q_3 \end{bmatrix}$$

$$\mathbf{L}_4 = \frac{1}{2}\begin{bmatrix} k_s + q_4 & k_s - q_4 \\ k_s - q_4 & k_s + q_4 \end{bmatrix} \qquad \mathbf{L}_5 = \frac{1}{2}\begin{bmatrix} k_s + q_5 & -\left(k_s - q_5\right) \\ -\left(k_s - q_5\right) & k_s + q_5 \end{bmatrix}$$

$$\mathbf{L}_6 = \frac{1}{2}\begin{bmatrix} k_s + q_6 & k_s - q_6 \\ k_s - q_6 & k_s + q_6 \end{bmatrix}$$

$$\mathbf{K} = \begin{bmatrix} \mathbf{L}_1 + \mathbf{L}_3 + \mathbf{L}_6 & -\mathbf{L}_3 & -\mathbf{L}_1 & -\mathbf{L}_6 \\ -\mathbf{L}_3 & \mathbf{L}_2 + \mathbf{L}_3 + \mathbf{L}_4 & -\mathbf{L}_4 & -\mathbf{L}_2 \\ -\mathbf{L}_1 & -\mathbf{L}_4 & \mathbf{L}_1 + \mathbf{L}_4 + \mathbf{L}_5 & -\mathbf{L}_5 \\ -\mathbf{L}_6 & -\mathbf{L}_2 & -\mathbf{L}_5 & \mathbf{L}_2 + \mathbf{L}_5 + \mathbf{L}_6 \end{bmatrix}$$

CHAPTER 2 ROLLING ROBOT – KINEMATIC BEHAVIOR DESCRIPTION

2.1 Introduction

The present section describes the kinematic behavior of the rolling robot. The first step is describing the geometry in terms of parameters which can be modified in order to set different geometry configurations. The equations of movement, velocity and acceleration will be obtained and also the trajectory of the robot will be predicted using a mathematical equations and known curves which fit with the geometrical transformations that the robot makes.

2.2 Basic Geometry Rolling Robot Description

The basic structure of the robot is based on large and width deformed bars, which shape spirals. These spirals are, in themselves, the body the structure, due they are the only component which are intended to support compression forces. In the following figure, we can observe the two general geometric characteristic of a spiral

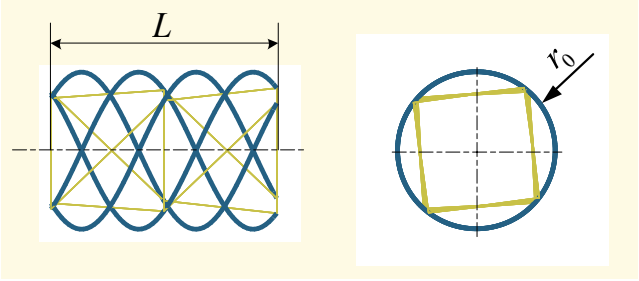

Figure 2-1 Basic Geometric Characteristic

These two geometric characteristic are invariables for any case of deformations rotation and movements. They are called as follow:

L Robot length $[\mathrm{m}]$

r_0 Basic central radius $[\mathrm{m}]$

We can defined the robot length as the length between the two extremes of the robot, this dimension is invariable because, as we can see later, both extremes are limited by thin prestressed wires which acting as a tensile element inside the tensegrity structure. Additionally, the basic central radius make reference to the imaginary radius in the middle of the robot, this dimension is present along the robot when this roll in a straight line, otherwise, in order to make curved movement over a plane, the structure must change its geometry, which implies, in this particular case, a variation on the radius along the length of the robot, making this a cone shape.

The basic structure of the bar members is a spiral, which shape a cylinder along its length. If we fix system of reference in the middle of the robot and at its left side, we can describe the geometry of the basic spiral.

$$ {}^1\vec{r}_s = \begin{bmatrix} s_{x1} \\ s_{y1} \\ s_{z1} \end{bmatrix} = \begin{bmatrix} r_0 \cos(\varphi) \\ \dfrac{L\varphi}{\pi} \\ r_0 \sin(\varphi) \end{bmatrix} \quad \varphi \in [-\pi;\ \pi] \tag{2.1} $$

Where:

s_{x1}, s_{y1}, s_{z1} Spiral shape equations.

${}^1\vec{r}_s$ Position vector of the spirals in the system O_1

$O_1 x_1 y_1 z_1$ Basic system of coordinates for the robot

φ Angle in the plane $x_0 - z_0$ respect the axis x_0 $[\mathrm{rad}]$

The system $O_1 x_1 y_1 z_1$ is the basic system from which the basic geometry of the robot is described, also it is necessary to create an additional coordinate system attached to the

origin of the system $O_1x_1y_1z_1$; around which the basic system of the robot rotates. This will be the system $O_0x_0y_0z_0$ and it is coincident with O_1. The system O_1 is allow to rotate to rotate around the axis x_0 and y_0.

$O_0x_0y_0z_0$ Referential coordinate system of the robot

In order to depict these equations over the plane $x_1 - z_1$, also the angle φ, the following figure shows the basic shape of the cross section of the robot:

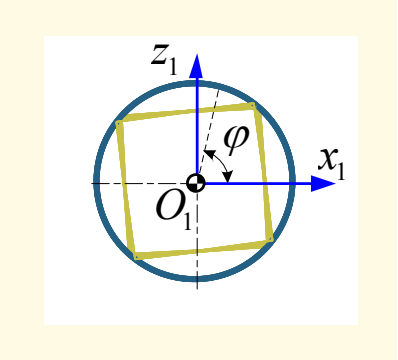

Figure 2-2 Cross section of the robot and system of reference

Also in the plane $y_1 - z_1$, the frontal view is depicted:

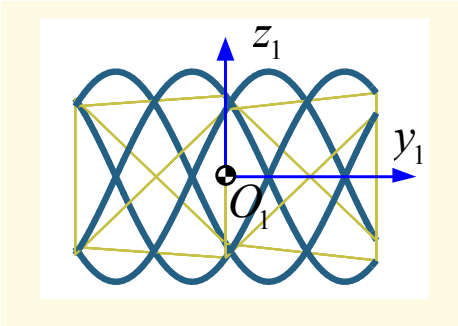

Figure 2-3 Frontal view of the robot and system of reference

2.3 Shape Robot Parameters

From the basic spiral the complete shape of the robot is generate. The complete geometry depends of some parameters, which determine the exact geometry. Each of the will be treated on the following sections:

2.3.1 Number of Spiral

The complete structure is a set of spirals which are rotated each other a fixed angle. This angle can be observed on the plane $x_o - z_0$. The number of spiral means the number of equal parts, in which, the circular cross section of the basic spiral is divided. Mathematically, we can define this as follow:

$$\vartheta = \frac{2\pi}{n_S} \tag{2.2}$$

Where

n_S Number of spirals of the robot

ϑ Angular gap between spirals $[\text{rad}]$

An example, when the number of spiral is four, can be observed in the following figure:

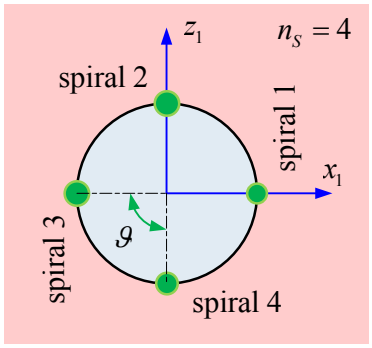

Figure 2-4 Distribution of spirals according with the number of them

In order to describe the geometry in term of equations, it is useful to apply Eulerian rotation matrix. Each of these spirals is exactly as the base spiral with the only difference that they are rotated around the y_1 axis an angle ϑ already defined and also and initial angle φ_0 which is an starting value for the rotation around y_0. Referring the entire spirals to the system $O_1x_1y_1z_1$, the following equation is valid for all the cases of number of spiral minors that 360 spirals.

$$
{}^{1}\begin{bmatrix} {}^{1}x_{sm} \\ {}^{1}y_{sm} \\ {}^{1}z_{sm} \end{bmatrix} = \begin{bmatrix} \cos\left(\varphi_0 + \vartheta(m-1)\right) & 0 & \sin\left(\varphi_0 + \vartheta(m-1)\right) \\ 0 & 1 & 0 \\ -\sin\left(\varphi_0 + \vartheta(m-1)\right) & 0 & \cos\left(\varphi_0 + \vartheta(m-1)\right) \end{bmatrix} \begin{bmatrix} s_{x1m} \\ s_{y1m} \\ s_{z1m} \end{bmatrix} \quad m \in [1, n_S] \tag{2.3}
$$

Where:

$^{1}x_{sm}, {}^{1}y_{sm}, {}^{1}z_{sm}$ Coordinates equations of the m – spiral in the system O_1

φ_0 Initial rotate angle around y_1 axis $[\text{rad}]$

The super index in the left indicates the reference system which the element is related.

The following figure is the generated geometry for $n_S = 3$ and $\varphi_0 = 0$. The other parameters are $r_0 = 1$ m, $L = 145/50$ m

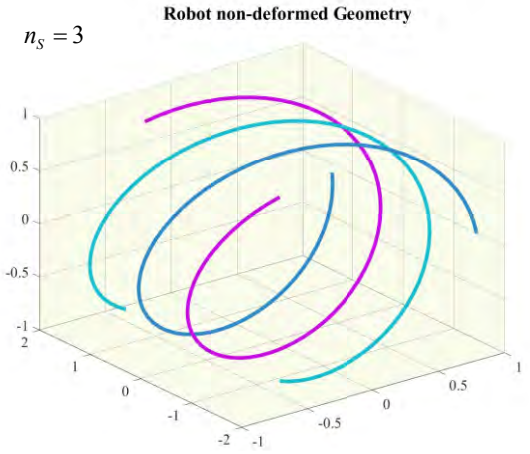

Figure 2-5 Robot non – deformed geometry

2.3.2 Developing angle

In the Figure 2-5, the spirals have developed a completed revolution, it means the angle φ in their geometrical equations is in the range between $-\pi$ and π. The maximum value of this range is called as developing angle. Despite this value does not interferes directly in the kinematic equations, it determines the length of the bar curved element and also the distributions of the masses along the y axis due the length is invariable and the beginning and end plane of the spiral muss be contained in this dimension. As consequence of this, the moment of inertia is affected due the distribution of masses

changes. The following figure shows a generated geometries for $n_S = 3$, $\varphi_0 = 0$, $r_0 = 0{,}1$ m, and $L = 145/500$ m with different developing angle and their principal mass inertial moment along the three axis respect their center of gravity:

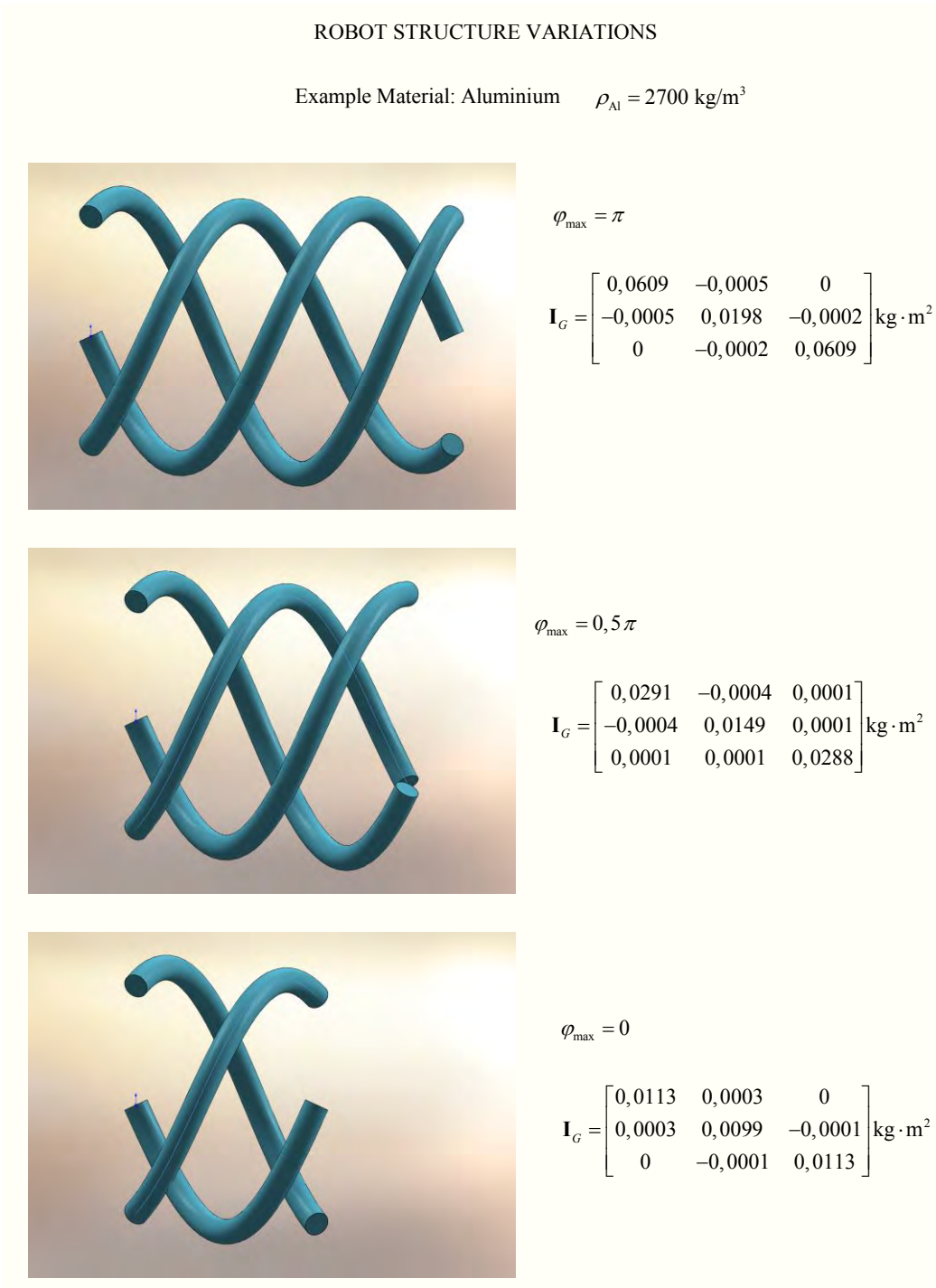

Figure 2-6 Variations of the developing angle on the robot structure

Where:

$\mathbf{I}_G$ Tensor of mass moment of inertia respect center of gravity $\left[\mathrm{kg}\cdot\mathrm{m}^2\right]$

$\varphi_{\max}$ Developing angle of the spiral $\left[\mathrm{rad}\right]$

The equations of the mass moment of inertia will be treated in further chapter, but in this case, it is useful to notice that it vary according the developing angle of the spiral structure.

2.4 Movement Equations

Once the robot geometry is complete defined, the movement can be described, but, in fact, when we refer to the movement we have to make reference to a specific point of the robot and also point the system of reference from which the movement is described.

Due the robot has a unknown trajectory, it could be impossible to set all the movement equations if we do not fix some parameters in order to know the path the robot is going to follow. For this reason, we start this section explaining the geometrical change on the robot structure and the effects it has in the movement of it; once it is clear and with the help of the auxiliary coordinate systems, the movement equation will be described.

2.4.1 Geometrical Change of the Robot

The robot would describe a straight path if it does not change it geometry due it is a cylinder and it only rolls around its axis of symmetry. The challenge of this new approach of structure is obtain a curved trajectory transforming the cylinder geometry into a conical geometry through variations in the internal stress of the element of the structure.

In an interval of the path, the structure begins to transform from a cylindrical into a conical form; the conical form has a parameter called conicity, this geometrical parameter is a relationship between difference of the internal and external radius and the length of the robot. In the following figure the concept is explained:

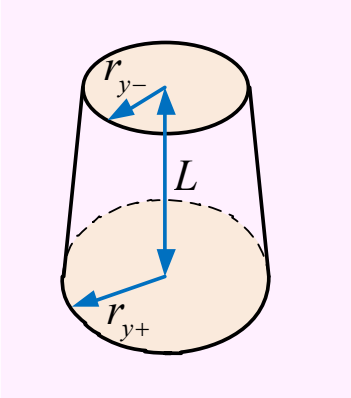

Figure 2-7 Conicity

Where:

r_{y+} Radius located on y_1^+ in the robot $[\mathrm{m}]$

r_{y-} Radius located on y_1^- in the robot $[\mathrm{m}]$

Also the conicity will be considered as follow:

$$C_R = 2\frac{r_{y+} - r_{y-}}{L} \tag{2.4}$$

Where:

C_R Conicity of the robot

According with this definition, the positive values of conicity are which the small radius is in the right face pointing out of the center of curvature of the trajectory.

Following with this idea, in a determined interval of time, the robot become from a null or from a known value of conicity to another desired value of conicity, it means the conicity has a rate of change. To use this geometrical parameter, it is better referring it as an angle:

$$\chi = \arctan\left(\frac{C_R}{2}\right) = \arctan\left(\frac{r_{y+} - r_{y-}}{L}\right) \tag{2.5}$$

Where:

χ Conicity angle $[\text{rad}]$

Due this conicity, the radius varies along the length of the robot; this variation will be treated as a lineal relation which can be watched in the following figure:

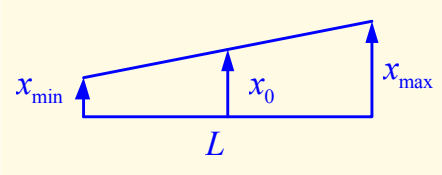

Figure 2-8 Robot's radius variation

If the value of the angle φ is in the range from $[0;2\pi]$ the equation which gives the value of the radius on each point of the robot is the following:

$$r_R(t) = r_0\left(1 - \frac{LC_R\varphi}{4\pi r_0}\right) \tag{2.6}$$

With this relation, the equation (2.1) becomes:

$${}^1\vec{r}_{sm}(t) = \begin{bmatrix} s_{x1m} \\ s_{y1m} \\ s_{z1m} \end{bmatrix} = \begin{bmatrix} r_R(t)\cos(\varphi) \\ \frac{L\varphi}{\pi} \\ r_R(t)\sin(\varphi) \end{bmatrix} \quad \varphi \in [-\pi;\ \pi] \tag{2.7}$$

${}^1\vec{r}_{sm}(t)$ Position vector of each point over the spirals in the system O_1 $[\text{m}]$

Further in this section, we will refer again to this angle, but, in this point, it is useful to highlight that this conicity angle describes a curvature radius:

$$R_K = \frac{r_0}{\sin(\chi)} \tag{2.8}$$

R_K Radius of curvature of the cone $[\text{m}]$

In order to have a refer point in the robot, we refer the curvature radius from the center of the robot to the surface of the basic central circumference, which is a circle with center contained in the y_0 axis. This idea is depicted in the following figure:

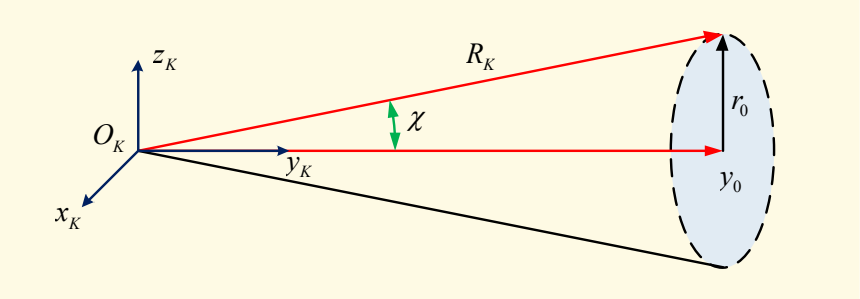

Figure 2-9 Description of the center of curvature of the center of the robot

$O_K x_K y_K z_K$ Coordinate system attached to the center of curvature

The system $O_K x_K y_K z_K$ is rotational only around axis z_K; also, the center of curvature is moving constantly, it is not fixed to a specific to point. For this reason, it is difficult to set equation which can predict the trajectory of the center of the robot, and we have to appeal to known mathematical relations which relate the curvature radius with another parameter. The control of the function and the prediction of the trajectory will be treaded in further in this chapter, after the equation of the movement and its parameter are described.

2.4.2 Movement Parameter

As it is expressed in the equations (2.3) and (2.1), all the spirals are rotated copies of a basic spiral, the range of the angle which describes this basic spiral defines the position of the system from we start to describe the movement. Due the movement is a rotation not only when the robot has a cylindrical shape, but also when it has a conical shape; we will control the change of geometry and the length of travel the robot will make, through the number of revolutions that the robot performs. This parameter is easy to control and measure, but it will give us a way to predict the trajectory due we can know, previously, the length of the curved path segment which is used to determine the clothoid parameter.

To refer to this parameter we are going to use an accumulated variable with save the total value of the rotated angle. In the following figure there is an explanation of this idea

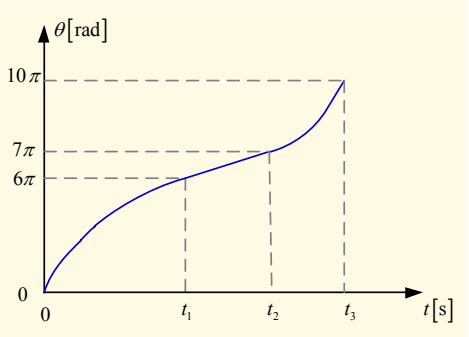

Figure 2-10 Schematic graphic rotated angle vs. time

Where:

θ Accumulated rotated angle θ [rad]

According with the figure, from 0 to 6π there is a decreasing angular speed, from 6π to 7π there is a constant angular speed and from 7π to 10π the angular speed is increasing. It means, the description of the movement is piecewise and the limits between the segments is the value of the accumulated rotated angle θ.Also, it works for the conicity; the segments with increasing, decreasing and keeping conicity value are limited also for the variable θ. The way that the conicity varies is constant, it means, there is a lineal correspondence between the conicity and the accumulated rotated angle. This can be observed in the following figure

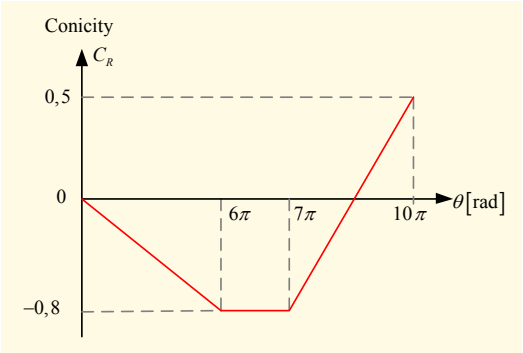

Figure 2-11 Schematic graphic rotated angle vs. theta

Although, it does not work for the conicity angle χ, due the relation between the conicity value and its conicity is a non – linear function; however, due the small values of the conicity, it can be approximated to a lineal behavior.

The approximation of the conicity angle to a lineal function it is useful to avoid to have an angular acceleration for the conicity angle, which will difficult the equations movement unnecessarily. The proximity of the lineal approximation and the real behavior of the conicity angle, when the conicity value starts from 0 and end in 0.7, can be watched in the following figure:

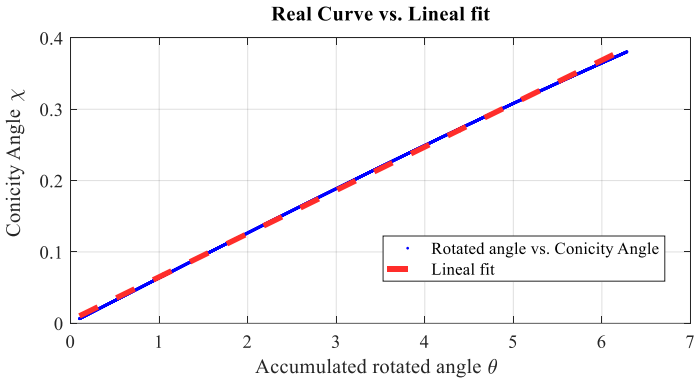

Figure 2-12 Real curve vs. Lineal fit for the conicity angle

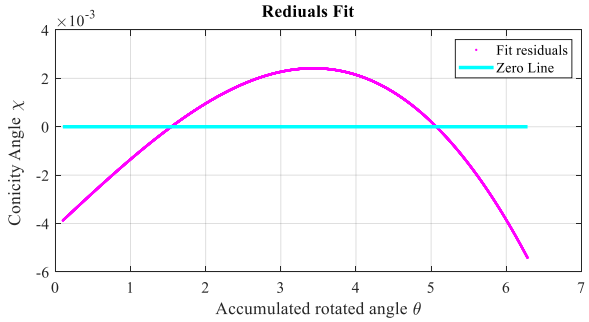

Figure 2-13 Residuals of the fit for the conicity angle

2.4.3 Rotations of the robot

The robot, due the geometrical changes it suffer, has a rotations around the three axis related to the system $O_0x_0y_0z_0$, which is rotational system, only around axis z_0,attached to the center of the robot. We will denominate the rotations angles as follow:

$\phi(t)$ **Roll angle**, rotation around x_0 $[\text{rad}]$

$\theta(t)$ **Pitch angle**, rotation around y_1 $[\text{rad}]$

$\psi(t)$ **Yaw angle**, rotation around z_K or parallel axis $[\text{rad}]$

The value of the pitch angle is equal to the value of the accumulated rotated angle described previously. In the following figure this angles will be described:

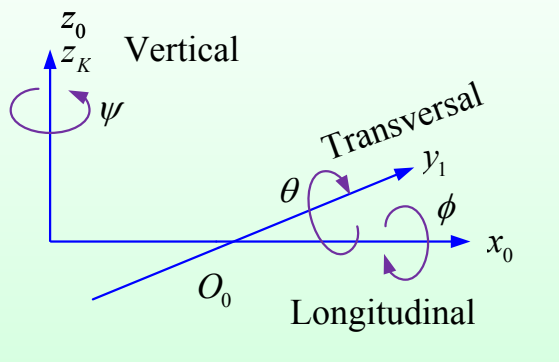

Figure 2-14 Rotation Angles

The axis x_0 remains oriented to the travel direction of the robot, the axis y_0 transversal to the travel directions and as a symmetry axis, and the axis z_0 to the vertical direction of the plane; additionally, we have to establish an inertial system from which the displacement will be described; this system $O_F X_F Y_F Z_F$ is establish as origin of the plane over the robot rolls.

$O_F X_F Y_F Z_F$ Inertial system of reference fix in the origin

The transformation matrix from O_0 to O_1 is the product of two transformation matrix due the three rotations the robot performs:

- Rotation around axis y_1

This rotation produces the rolling movement of the robot; it is defined by the following matrix, also it is intended that all the angles a function of the time, so the indication (t) will be retired in order to simplify the expressions:

$$ {}^{01}\mathbf{T}_y(t) = \begin{bmatrix} \cos(\theta) & 0 & \sin(\theta) \\ 0 & 1 & 0 \\ -\sin(\theta) & 0 & \cos(\theta) \end{bmatrix} \tag{2.9} $$

${}^{01}\mathbf{T}_y(t)$ Transformation matrix from O_0 to O_1 for turn around y_1

In this case, the rotation is around the axis of symmetry of the robot, which is always the y_1 axis. We keep the same system, but this rotation also varies the orientation of x_1 and z_1.

- Rotation around axis x_0

This rotation is explained in the following figure:

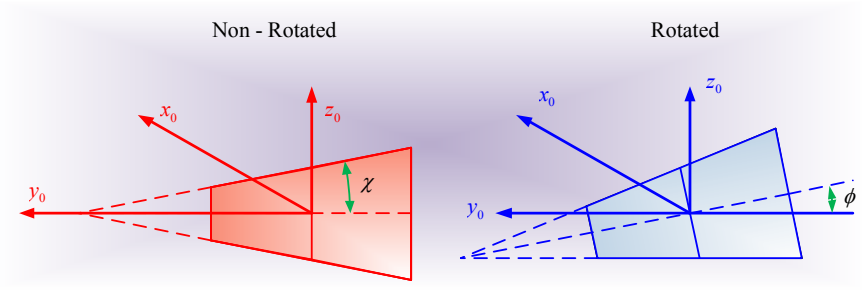

Figure 2-15 Rotation around axis x_0

According with the figure, the conicity angle is equal to the roll angle for geometry numerically:

$$\phi(t) = \chi(\theta(t)) \tag{2.10}$$

Finally, the rotation is calculated by the following matrix:

$$^{01}\mathbf{T}_x(t) = \begin{bmatrix} 1 & 0 & 0 \\ 0 & \cos(\phi) & -\sin(\phi) \\ 0 & \sin(\phi) & \cos(\phi) \end{bmatrix} \tag{2.11}$$

$^{01}\mathbf{T}_x(t)$ Transformation matrix from O_0 to O_1 for turn around x_0

The definition of the system O_0 is not located over the plane; also the result of this transformation requires a vertical displacement in order to locate the robot over the plane. The rolling plane is given by the X_F and Y_F. This displacement can be watched in the following figure:

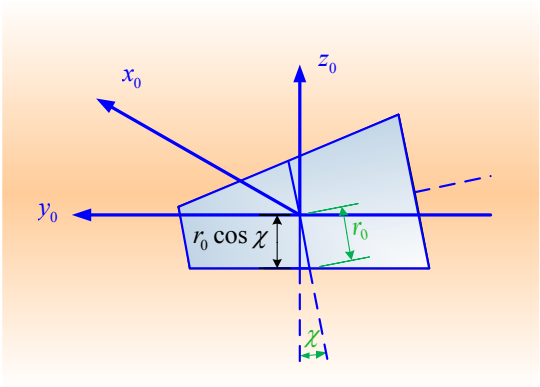

Figure 2-16 Vertical displacement for planning position of the robot

The vertical displacement is given for the following relation:

$$d_z(t) = r_0 \cos(\phi) \tag{2.12}$$

Where:

d_z Vertical displacement $[\mathrm{m}]$

- Rotation around axis z_K

The angle ψ is also responsible for the curved movement that the robot describes; this angle is the orientation of the axis x_0 and y_0 respect the system XYZ. Due the axis z_0, z_K and Z_F remains always parallel, the value of ψ is also valid for the rotation of the system $O_K x_K y_K z_K$ around z_K. In the following figure, we can appreciate that the robot turn around the z_K axis which is located in the center of curvature of the conical shape.

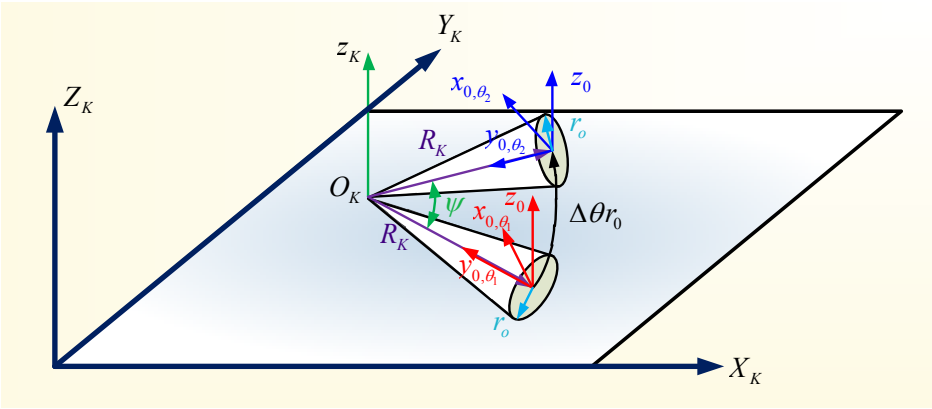

Figure 2-17 Rotation around z_K

The value of the angle ψ is just the angle that form the arc created by the two curvature radius separated a distance which is the basic radius of the robot multiplied by the change of the angle θ which is the turning which moves the robot.

Due it depends on the change of the angle θ between intervals of time, the value of the angle ψ will be calculated as an accumulated variable

$$\psi(t) = \psi(t-1) + \frac{r_0 \Delta\theta}{R_K(t)} \tag{2.13}$$

Where:

$\Delta\theta$ Variation of the angle θ $[\text{rad}]$

According with the Figure 2-17, the rotation center of the robot is the center of curvature; also, in each instant, the direction of the axis x_0 and y_0 are changing.

Finally, the rotation is calculated by the following matrix:

$$^{0F}\mathbf{T}_Z(t) = \begin{bmatrix} \cos(\psi) & \sin(\psi) & 0 \\ -\sin(\psi) & \cos(\psi) & 0 \\ 0 & 0 & 1 \end{bmatrix} \tag{2.14}$$

$^{0F}\mathbf{T}_Z(t)$ Transformation matrix turning around z_K

This matrix transforms the coordinates into a system, which is parallel to the system $O_F X_F Y_F Z_F$.

2.4.4 Displacement of the robot

The upper part of the equation (2.13) is the displacement of the robot over the plane. This displacement must be discomposed on the axis X_F and Y_F in order to determine the movement of the variation of the coordinates of the robot over the plane. In the following figure it can be watched:

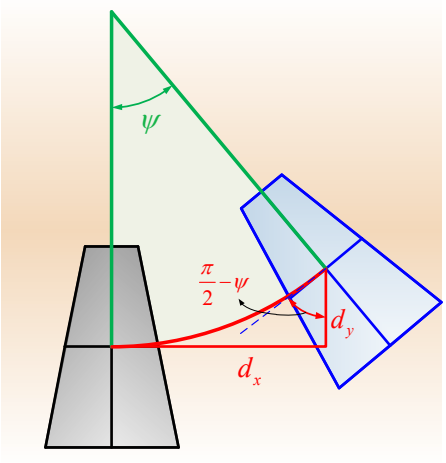

Figure 2-18 Displacement of the robot over the plane

For the equations of this displacement, it is necessary to pay attention to the direction of the turning around the vertical axis, from the equation (2.14), to generate a rotation in the direction depicted in the Figure 2-18, which is a positive sense for turning around it axis, the sign of the angle ψ must be negative, due the transformation are in inverse way, it means, it comes from the rotated system to the non – rotated system fixed in the origin of the plane.

Due the displacement is calculated for the arc developed of the robot described for its rotation at each interval of time, it means, it depends on the change of the angle θ,the value of the displacement along the axis on the plane will be calculated as an accumulated variable

Then:

$$d_x(t) = d(t-1) + r_0\ \Delta\theta\ \sin\left(\frac{\pi}{2} - \psi(t)\right) \tag{2.15}$$

$$d_y(t) = d(t-1) - r_0\ \Delta\theta\cos\left(\frac{\pi}{2} - \psi(t)\right) \tag{2.16}$$

Where:

d_x Displacement along X_F axis $[\mathrm{m}]$

d_y Displacement along Y_F axis $[\mathrm{m}]$

These relationships are originated due the cosines for values higher than $\pi/2$ are negative and the sinus is positives. Also the angle $(\pi/2-\psi)$ is the angle present between the arc displaced at that interval of time and a vertical line parallel to the axis Y_F

2.4.5 Gathering of equations

With all the turnings and displacement declared, the following equivalence can be established in order to determine the position of each node of each spiral of the robot during it movement. In order to describe the equations in a sequential way, they will be described as a transformation between systems:

- Transformation from O_1 to O_0

Developing the equation (2.7):

$$ {}^1\vec{r}_{sm}(t) = \begin{bmatrix} s_{x1} \\ s_{y1} \\ s_{z1} \end{bmatrix} = \begin{bmatrix} r_R(t)\cos(\varphi) \\ \dfrac{L\varphi}{\pi} \\ r_R(t)\sin(\varphi) \end{bmatrix} \quad \varphi \in [-\pi;\ \pi] \tag{2.17} $$

Also,(2.3), (2.9),(2.11) and introducing (2.17), we have

$$ {}^0\vec{r}_{sm}(t) = \begin{bmatrix} {}^0x_{sm} \\ {}^0y_{sm} \\ {}^0z_{sm} \end{bmatrix} = {}^{01}\mathbf{T}_x(t)\,{}^{01}\mathbf{T}_y(t)\,{}^1\vec{r}_{sm}(t) \quad m \in [1, n_S] \tag{2.18} $$

${}^0x_{sm}, {}^0y_{sm}, {}^0z_{sm}$ Coordinates equations of the m – spiral in the system O_0

${}^0\vec{r}_{sm}(t)$ Position vector of each point over the spirals in system O_0 $[\mathrm{m}]$

- Transformation from O_0 to O_F

First, we have to displace the system O_0 to the same level of the system O_F and then rotate it and finally displace it another time. Taking the equations (2.12), (2.14), (2.15) and (2.16), we find the coordinates of each point of the robot referred to the system $O_F X_F Y_F Z_F$

$$\begin{bmatrix} {}^{F}X_{sm} \\ {}^{F}Y_{sm} \\ {}^{F}Z_{sm} \end{bmatrix} = \begin{bmatrix} d_x(t) \\ d_y(t) \\ d_z(t) \end{bmatrix} + {}^{F0}\mathbf{T}_Z(t) \begin{bmatrix} {}^{0}x_{sm} \\ {}^{0}y_{sm} \\ {}^{0}z_{sm} \end{bmatrix} \quad m \in [1, n_S] \tag{2.19}$$

The equations (2.17), (2.18),(2.19) are a resume of the movements of the robot for all conditions of change of geometry and considering an entire number of spirals. The following section will apply the clothoid to determine the trajectory of the robot, which can be used for control purposes.

2.5 Prediction of the trajectory of the robot in variable curvature radius

The parameter used to the movement of the robot described in the section 2.4.2, can be used, also, to predict the trajectory for all cases of conicity.

When the conicity constant is, the trajectory is a circle around the center of curvature; in other cases, the trajectory describes another figure over the plane due the large range of the curvature radius and variable position of the center of curvature. For this reason, the task to find a geometrical relation becomes impossible if we do not assume something or we have the capability to control something in the movement of the robot.

The first important thing to notice that the conicity angle and the curvature radius have a limit value given by:

$$\lim_{\chi \to 0} \frac{r_0}{\sin(\chi)} = \infty \tag{2.20}$$

$$\lim_{\chi \to \frac{\pi}{2}} \frac{r_0}{\sin(\chi)} = r_0 \tag{2.21}$$

It means that when the robot describes a straight path, the curvature radius tends to infinity; also, as this grows the radius becomes smaller with a limit in r_0 as we can see in the following figure.

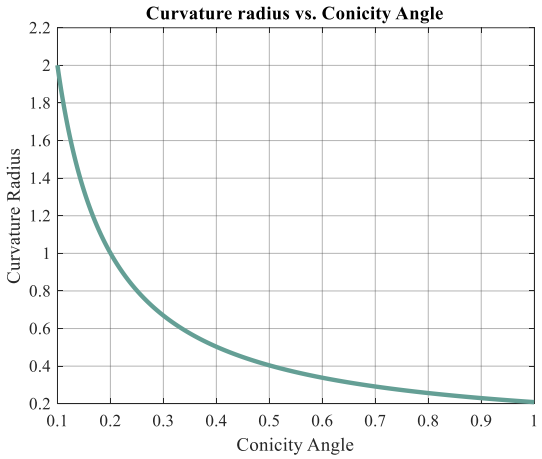

Figure 2-19 Conicity angle vs. Curvature radius

At this point, it is necessary to introduce a relationship between the radius of curvature and another dimension of the curve, which could be the traveled distance on the trajectory. These both dimensions are related for the well – known curve **Clothoid** which is known in the world of railway path design as a transition curve.

This curve is defined mathematically with the following equation:

$$R_K(s) \cdot s = A^2 \tag{2.22}$$

Where:

A	Coefficient of the Clothoid
s	Traveled distance over the curve $[\mathrm{m}]$

The Clothoid set a lineal relationship between the radius of curvature and the traveled distance. An example of this curved is drawn in the following figure:

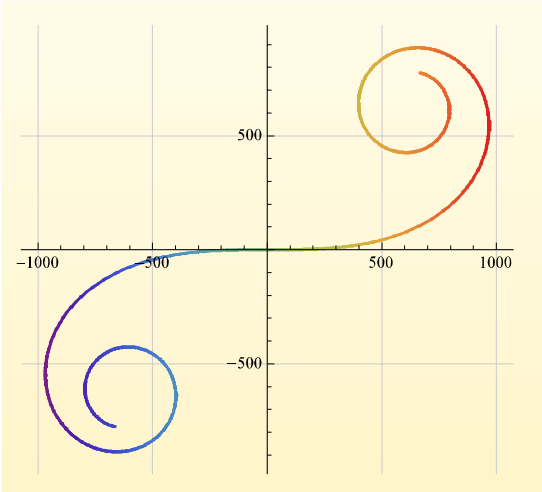

Figure 2-20 Clothoid with A = 700

The equation (2.22) can be parameterized through mathematical deductions which can be found in [4], the final results of these operations are the equations for the coordinates x and y as a function of the traveled distance over the curve:

$$x(s)-x(s_0)=\int_{s_0}^{s}\cos\left(\frac{s^2}{2A^2}\right)ds \tag{2.23}$$

$$y(s)-y(s_0)=\int_{s_0}^{s}\sin\left(\frac{s^2}{2A^2}\right)ds \tag{2.24}$$

If we substitute $s_0=0$ and $[x(s_0);y(s_0)]=[0;0]$ in (2.23) and (2.24):

$$\vec{r}=\begin{bmatrix}x(s) & y(s)\end{bmatrix}=\left[\int_{s_0}^{s}\cos\left(\frac{s^2}{2A^2}\right)ds \quad \int_{s_0}^{s}\sin\left(\frac{s^2}{2A^2}\right)ds\right] \tag{2.25}$$

Finally, solving the integrals of the relation (2.25), we obtain:

$$\vec{r}(s)=[x(s);y(s)]=A\sqrt{\pi}\left[\text{FresnelC}\left(\frac{s}{A\sqrt{\pi}}\right);\text{FresnelS}\left(\frac{s}{A\sqrt{\pi}}\right)\right] \tag{2.26}$$

Fresnel cosine and Fresnel sinus are complex mathematical function which can be solved only through numerical integration. Sometimes both functions of Fresnel are approximated through Taylor's series, but which implies an approximation mistakes

which we must take in account for predict trajectories. For the scopes of this work, these functions will be treated numerically.

For the application of this curve, it must be necessary to know the initial and final values of conicity, therefore, conicity angle; sometimes these values can start on a positive value and end in a negative value or start on zero. The principal task is determining the value of the parameter A of the clothoid. We start calculating the derivate of the equation (2.25):

$$\frac{d\vec{r}(s)}{ds}: \quad \vec{T}(s)=\hat{t}_C(s)=\left[\cos\left(\frac{s^2}{2A^2}\right);\ \sin\left(\frac{s^2}{2A^2}\right)\right] \tag{2.27}$$

Where:

$\hat{t}_C$ Unitary tangent vector of the clothoid

$\vec{T}(s)$ Tangent vector of the clothoid

For definition of derivative, the equation (2.27) gives the tangent vector at each point of the clothoid; following, we obtain the normal vector calculating the derivate another time:

$$\frac{d\vec{T}(s)}{ds}: \quad \vec{N}(s)=\frac{s}{A^2}\left[-\sin\left(\frac{s^2}{2A^2}\right);\cos\left(\frac{s^2}{2A^2}\right)\right] \tag{2.28}$$

And its unitary vector

$$\hat{n}(s)=\frac{\vec{N}(s)}{\left|\vec{N}(s)\right|}=\left[-\sin\left(\frac{s^2}{2A^2}\right);\cos\left(\frac{s^2}{2A^2}\right)\right] \tag{2.29}$$

Where:

$\hat{n}(s)$ Unitary normal vector of the clothoid

$\vec{N}(s)$ Normal vector of the clothoid

Additionally, we have to control the way the conicity angle varies with an angular speed which will be considered constant In order to relate the conicity value at the starting or final point with the traveled distance over the curve, we can use the following rule:

$$\text{sign}(s)=\begin{cases}\text{negative} & \text{if } \sin(\chi)>0\\ \text{positive} & \text{if } \sin(\chi)<0\\ 0 & \text{otherwise}\end{cases} \tag{2.30}$$

It means that if the conicity is negative, the value of the traveled distance over the curve has a negative sign, otherwise it is positive or zero if there is not conicity. This definition is useful to avoid mistakes at the moment to define the sense of the curve, due as we can see in the Figure 2-20, the clothoid is defined in both directions of the horizontal axis, even it can be reflected along the vertical axis only varying the sign inside the Fresnel functions. The reflected clothoid is described by the following equations:

$$[x(s);y(s)]=A\sqrt{\pi}\left[\text{FresnelC}\left(\frac{s}{A\sqrt{\pi}}\right);-\text{FresnelS}\left(\frac{s}{A\sqrt{\pi}}\right)\right] \tag{2.31}$$

Graphically:

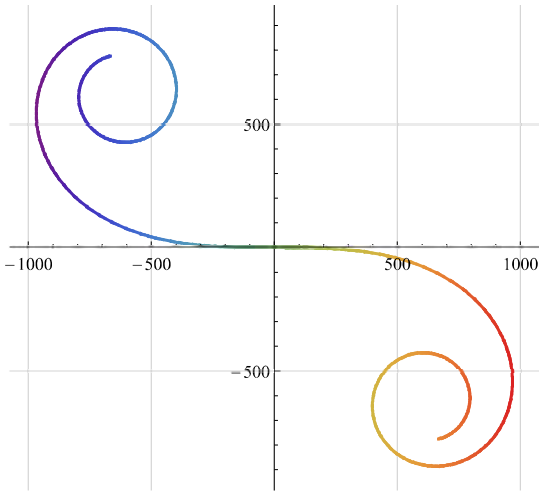

Figure 2-21 Inverted Clothoid

The application of this curve to the predictions of trajectories in conditions of variable conicity will be made with an example. For an trajectory composed by two intervals in terms of θ from 0 to $1,5\pi$ and $1,5\pi$ to 9π, the conicity varies from 0 to 0.5 and from 0,5 to $-0,7$ respectively. With the results that the equations (2.17), (2.18) and (2.19), the trajectory obtained for the given condition is depicted in the following figure:

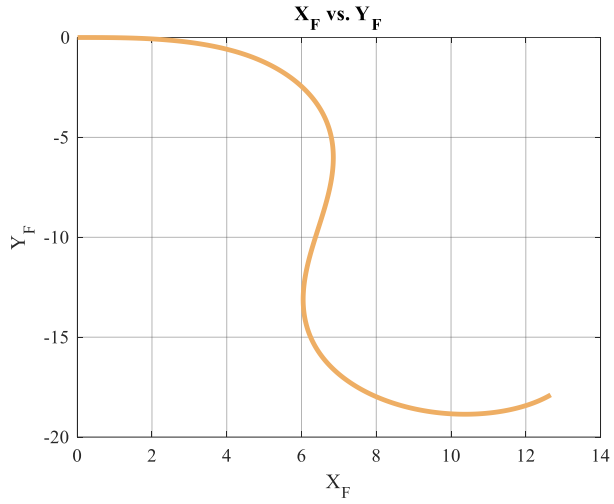

Figure 2-22 Example trajectory

In order to apply a non – inverted clothoid, we will determine the parameters of the second segment of the trajectory. The first step is knowing the length of the curve that the middle of the robot will travel, as it is calculated in the previous calculus for the displacement of the system O_0, we will use the basic radius to get this measure:

$$|\Delta s| = (9-1,5)\pi r_0$$

So, we can express it in a general way as follow:

$$|\Delta s| = (\theta_f - \theta_0) r_0 \tag{2.32}$$

Where:

Δs	Variation of the values of length of traveled curve inside the fitting clothoid $[\text{m}]$
θ_0	Starting value of θ in the clothoid $[\text{rad}]$
θ_f	Final value of θ in the clothoid $[\text{rad}]$

With $r_0 = 1$ m, we get:

$$|\Delta s| = 23,5619 \text{ m}$$

The relation (2.32) expresses the absolute value of the difference between traveling distance over the clothoid. The exactly value is given by:

$$\Delta s = s_f - s_0$$

Where:

s_0 Starting value of traveling distance over the clothoid in the clothoid $[\mathrm{m}]$

s_f Final value of traveling distance over the clothoid in the clothoid $[\mathrm{m}]$

According with the rule given in the equation (2.30), the traveled distance over the clothoid can be positive or negative depending on the sign of the conicity.

The following step is find the clothoid parameter and the starting value of traveled curve inside the clothoid; then, we have to calculate the initial and final conicity angle and the curvature radius using the equations (2.5) and (2.8)

$$\chi_0 = 0,244979 \text{ rad}$$

$$\chi_f = -0,358771 \text{ rad}$$

Where:

χ_0 Starting value of conicity angle in the clothoid $[\mathrm{rad}]$

χ_f Final value of conicity angle in the clothoid $[\mathrm{rad}]$

Then, we get the curvature radius:

$$R_{K0} = 4,12311 \text{ m}$$

$$R_{Kf} = -2,848 \text{ m}$$

Where:

R_{K0} Starting value of curvature radius in the clothoid $[\mathrm{m}]$

R_{Kf} Final value of curvature radius in the clothoid $[\mathrm{m}]$

Using the basic definition of the clothoid, equation (2.22), we find the parameter of the clothoid:

$$4{,}12311 \cdot s_0 = A^2 \tag{2.33}$$

$$-2{,}848 \cdot s_f = A^2 \tag{2.34}$$

As a logical result, in the equation (2.34) the value of s_f must be negative, it proofs the rule expressed in (2.30). Dividing (2.33) by (2.34), we find a relation between the end value and the starting value of the traveling distance over the clothoid:

$$\frac{s_0}{s_f} = -0{,}69074$$

Then, we have:

$$s_f + 0{,}690 s_f = 23{,}5619$$

Following the rule of the equation (2.30), s_f is negative:

$$s_f = -13{,}93585 \text{ m}$$

$$s_0 = 9{,}62605 \text{ m}$$

Finally, we find the coefficient of the clothoid:

$$A = 6{,}2999$$

The trajectory obtained through this procedure for this segment is depicted in the following figure:

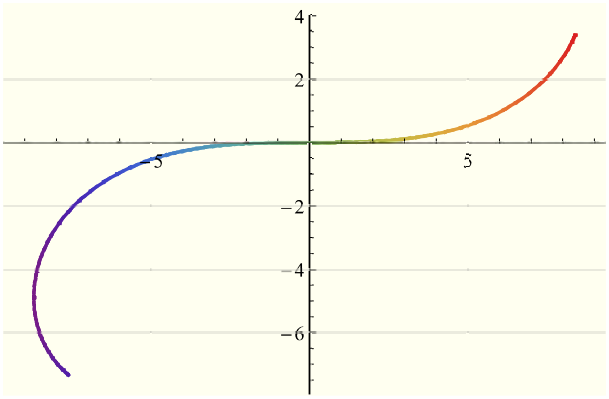

Figure 2-23 Resulting clothoid for movement prediction

This result must be connected with a circular segment or straight segment or another clothoid, this operation involves displacements and turnings which must be calculated using the information from the previous segment to which the obtained clothoid will be attached. Following with this idea, we have to determine the parameter for the first segment of the trajectory, but this segment has a significant different with the segment calculated previously, in which, the conicity decrease from $0,5$ to $-0,7$, but in the first segment it varies in opposite way, the conicity comes from 0 to 0,5, there is a change in the direction of the way that the sign of the radius of curvature changes, in consequence, it makes that the clothoid change its directions. Taking the previous example, if we calculate the clothoid for an interval of θ between 0 to $1,5\pi$, the conicity varies from 0 to 0,5.

Applying the calculus procedure explained before:

$$\Delta s = 1,5\pi \text{ m}$$

$$\chi_0 = 0 \text{ rad}$$

$$\chi_f = 0,24498 \text{ rad}$$

$$R_{K0} = \infty$$

$$R_{Kf} = 4,12311 \text{ m}$$

$$s_0 = 0 \text{ m}$$

$$s_f = 1,5\pi \text{ m}$$

$$A = 4,407913126$$

The obtained clothoid with these parameters is showed in the following figure:

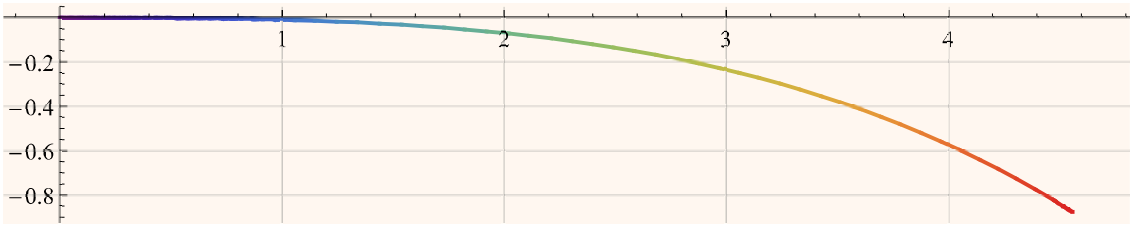

Figure 2-24 Resulting clothoid for the first segment example

This result, which is an inverted clothoid, fits with the result obtained using the equations (2.17), (2.18) and (2.19) depicted in the following figure:

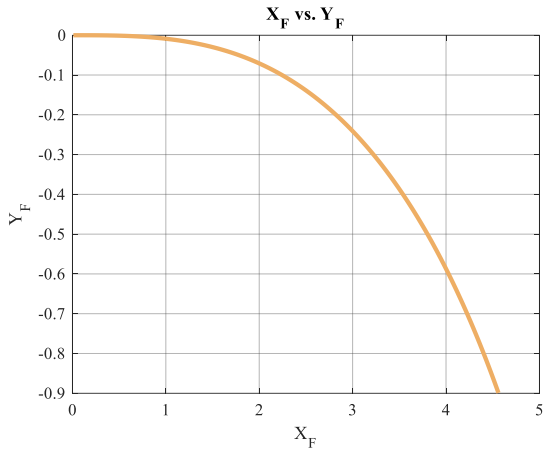

Figure 2-25 Movement for conicity variation from 0 to 0,5

For convenience we will calculate the normal unitary vector for the starting and last interval and of the first segment:

So, it is useful to show, that the unitary vector equation for the inverted clothoid is the following:

$$\hat{n}_I(s) = \left[-\sin\left(\frac{s^2}{2A^2}\right); -\cos\left(\frac{s^2}{2A^2}\right) \right] \tag{2.35}$$

$\hat{n}_I$ Unitary normal vector for inverted clothoid

Using the equation (2.35), we obtain:

$$\hat{n}_0(s) = \left[-\sin\left(\frac{0^2}{2(4,40791)^2}\right); -\cos\left(\frac{0^2}{2(4,40791)^2}\right) \right]$$

$$\hat{n}_0(s) = [-0,00997; -0,999]$$

$$\hat{n}_f(s) = \left[-\sin\left(\frac{(1,5\pi)^2}{2(4,40791)^2}\right); -\cos\left(\frac{(1,5\pi)^2}{2(4,40791)^2}\right) \right]$$

$$\hat{n}_f(s) = [-0,540861; -0,841112]$$

Where:

$\hat{n}_0$ Unitary normal vector at the starting point

$\hat{n}_f$ Unitary normal vector at the final point

Also the direction of the normal vector of the clothoid is almost coincident with the value of the cosines and sinus of the angle ψ at the final point of this segment

$$\hat{n}_\psi = \left[-\sin(\psi) \quad -\cos(\psi)\right] \tag{2.36}$$

Where:

$\hat{n}_\psi$ Unitary normal vector obtained by ψ angle

With: $\psi = 0,58075$

$$\hat{n}_\psi = \left[-0,54865 \quad -0,83605\right]$$

The percentage of error is:

$$\left[1,42\% \quad 0,605\%\right]$$

These percentages allow us to say the clothoid fits the results obtained with the equations developed previously for the movement of the robot.

Finally to connect the two segments, so we have to transform the equations of the second segment in order to be added. For this purpose, we calculate the unitary tangential vector of the last point of the first segment and the first point of the second segment. Also for the inverted clothoid the unitary tangential vector is expressed as follow

$$\hat{t}_{CI}(s) = \left[\cos\left(\frac{s^2}{2A^2}\right); -\sin\left(\frac{s^2}{2A^2}\right)\right] \tag{2.37}$$

$\hat{t}_{CI}(s)$ Tangential unitary vector for inverted clothoid

Then we have:

$$\hat{t}_{f1} = \left[0,84111 \quad -0,54086\right]$$

$$\hat{t}_{02} = \begin{bmatrix} 0,39263 & 0,91970 \end{bmatrix}$$

Where:

t_{f1} Tangential unitary vector of the last point of the first segment

t_{02} Tangential unitary vector of the first point of the second segment

And the tangency angles:

$$\xi_1 = \arctan\left(\frac{-0,54086}{0,84111}\right) = -0,57146 \text{ rad}$$

$$\xi_2 = \arctan\left(\frac{0,91970}{0,39263}\right) = 1,16731 \text{ rad}$$

Where:

t_{f1} Tangential unitary vector of the last point of the first segment

t_{02} Tangential unitary vector of the first point of the second segment

To ensure the continuity of the curves, both tangency angles must be equal, in consequence, the equations of the second segment will be rotated and then translated, in order to be connected to the first segment.

$$\Delta\xi = |\xi_2| - |\xi_1| \tag{2.38}$$

Where

$\Delta\xi$ Rotation angle for the clothoid

Finally, the displacement is calculated, for this, the coordinate of the last point of the first segment must be equal to the first point of the rotated second segment:

$$\begin{bmatrix}\Delta x\\ \Delta y\end{bmatrix} = A_1\sqrt{\pi}\begin{bmatrix}\text{FresnelC}\left(\dfrac{s_{f1}}{A_1\sqrt{\pi}}\right)\\ -\text{FresnelS}\left(\dfrac{s_{f1}}{A_1\sqrt{\pi}}\right)\end{bmatrix} - A_2\sqrt{\pi}\begin{bmatrix}\cos(\Delta\xi) & \sin(\Delta\xi)\\ -\sin(\Delta\xi) & \cos(\Delta\xi)\end{bmatrix}\begin{bmatrix}\text{FresnelC}\left(\dfrac{s_{02}}{A_2\sqrt{\pi}}\right)\\ -\text{FresnelS}\left(\dfrac{s_{02}}{A_2\sqrt{\pi}}\right)\end{bmatrix} \tag{2.39}$$

Finally we obtain the following trajectory:

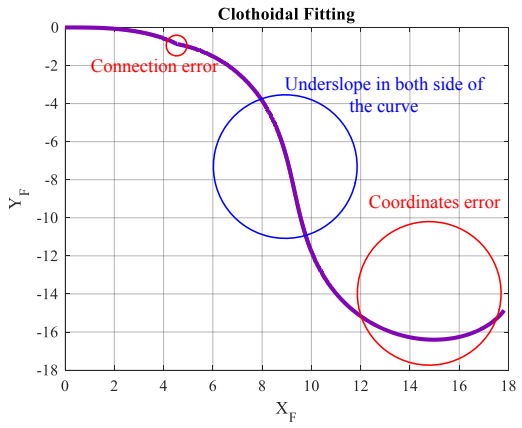

Figure 2-26 Clothoidal fitting and mistakes

Making a comparison between the Figure 2-22 and Figure 2-26, it is highlighted that there is mistakes in the clothoidal fitting. First, at the connection point between clothoids there is a mismatch in the tangential vector at these points; it can be solved finding a better determination process of the coefficient of the connecting clothoids. In the middle of the second segment, there is an underslope in both sides of the clothoid originated by the approximation process. Again, improving determination process of the coefficient of the connecting clothoids, but also, the mistakes could be reduced making the traveling distance over the curve shorter, it means reduce the value of Δs. Finally all the previous mistakes described are traduced in coordinate errors.

As a resume, we show the equations obtained for the trajectory using the clothoidal fitting in terms of θ:

For $\theta \in [0;1,5\pi]$

$$\begin{bmatrix} x_{C1} \\ y_{C1} \end{bmatrix} = A_1\sqrt{\pi}\begin{bmatrix} \text{FresnelC}\left(\dfrac{s}{A_1\sqrt{\pi}}\right) \\ -\text{FresnelS}\left(\dfrac{s}{A_1\sqrt{\pi}}\right) \end{bmatrix} \quad s \in [0,1,5\pi]$$

For $\theta \in [1,5\pi;\, 9\pi]$

$$\begin{bmatrix} x_{C2} \\ y_{C2} \end{bmatrix} = A_2\sqrt{\pi}\begin{bmatrix} \cos(\Delta\xi) & \sin(\Delta\xi) \\ -\sin(\Delta\xi) & \cos(\Delta\xi) \end{bmatrix}\begin{bmatrix} \text{FresnelC}\left(\dfrac{s}{A_2\sqrt{\pi}}\right) \\ -\text{FresnelS}\left(\dfrac{s}{A_2\sqrt{\pi}}\right) \end{bmatrix} - \begin{bmatrix} \Delta x \\ \Delta y \end{bmatrix} \quad s \in [-13,93585;\, 9,62605]$$

But the real advantage of this approach is the capability to have an equation or a piecewise equation which gives the position of the center of the robot, and in consequence of all the nodes within, as a function of the accumulated rotated angle θ, which can be translated in terms of time. Despite the approximation mistakes, which can be solved in further works, this approach offers a way to program the total trajectory of the robot; additionally, another principal difference between the results of this approach and the equations (2.17), (2.18) and (2.19) the lasts only give points, but not equations.

2.6 Velocity Equations

From the equations (2.17), (2.18) and (2.19), the velocity equations can be obtained through derivation process, but it means, taking in account all the behaviors we establish for the rotation angles.

We will divided the derivation process in two parts, from O_1 to O_0 and from O_0 to O_F

2.6.1 Derivation from O_1 to O_0

We start with the equation (2.18), so we can express the derivate as follow:

$$\frac{d^0 r_{sm}(t)}{dt} = \frac{d^0\left[{}^{01}\mathbf{T}_x(t)\,{}^{01}\mathbf{T}_y(t)\,{}^{1}r_{sm}(t)\right]}{dt} \quad m \in [1, n_S] \tag{2.40}$$

Also we can simplify the equation (2.18) and (2.40) making a unique transformation matrix:

$${}^{01}\mathbf{T} = {}^{01}\mathbf{T}_x(t)\,{}^{01}\mathbf{T}_y(t) \tag{2.41}$$

$${}^{01}\mathbf{T} = \begin{bmatrix} \cos(\theta) & 0 & \sin(\theta) \\ -\sin(\theta)\sin(\phi) & \cos(\phi) & \cos(\theta)\sin(\phi) \\ -\cos(\phi)\sin(\theta) & -\sin(\phi) & \cos(\theta)\cos(\phi) \end{bmatrix} \tag{2.42}$$

Where:

${}^{01}\mathbf{T}$ Transformation matrix from O_0 to O_1

Also using the equation of Poisson:

$${}^{0}\tilde{\boldsymbol{\omega}}_{10}(t) = {}^{01}\dot{\mathbf{T}}(t)\,{}^{01}\mathbf{T}^{\mathrm{T}}(t) \tag{2.43}$$

Also:

$${}^{1}\tilde{\boldsymbol{\omega}}_{10}(t) = {}^{01}\mathbf{T}^{\mathrm{T}}(t)\,{}^{01}\dot{\mathbf{T}}(t) \tag{2.44}$$

Where:

${}^{0}\tilde{\boldsymbol{\omega}}_{10}(t)$ Angular speed skew symmetric matrix of O_1 respect O_0 in system O_0 [rad/s]

${}^{1}\tilde{\boldsymbol{\omega}}_{10}(t)$ Angular speed skew symmetric matrix of O_1 respect O_0 in system O_1 [rad/s]

${}^{01}\dot{\mathbf{T}}(t)$ First derivate of the transformation matrix from O_0 to O_1

Making the mathematical operation, we obtain:

$${}^{01}\dot{\mathbf{T}}(t) = \begin{bmatrix} -\sin(\theta)\dot{\theta} & 0 & \cos(\theta)\dot{\theta} \\ \cos(\theta)\sin(\phi)\dot{\theta} + \cos(\phi)\sin(\theta)\dot{\phi} & -\sin(\phi)\dot{\phi} & \sin(\theta)\sin(\phi)\dot{\theta} - \cos(\theta)\cos(\phi)\dot{\phi} \\ -\cos(\theta)\cos(\phi)\dot{\theta} + \sin(\theta)\sin(\phi)\dot{\phi} & \cos(\phi)\dot{\phi} & -\cos(\phi)\sin(\theta)\dot{\theta} - \cos(\theta)\sin(\phi)\dot{\phi} \end{bmatrix} \tag{2.45}$$

Replacing in (2.44):

$$ {}^{0}\tilde{\boldsymbol{\omega}}_{10}(t)=\begin{bmatrix} 0 & -\sin(\phi)\dot{\theta} & \cos(\phi)\dot{\theta} \\ \sin(\phi)\dot{\theta} & 0 & -\dot{\phi} \\ -\cos(\phi)\dot{\theta} & \dot{\phi} & 0 \end{bmatrix} \tag{2.46} $$

$$ {}^{0}\vec{\omega}_{10}=\begin{bmatrix} \dot{\phi} \\ \cos(\phi)\dot{\theta} \\ \sin(\phi)\dot{\theta} \end{bmatrix} \tag{2.47} $$

Finally

$$ {}^{0}\vec{v}_{sm}(t)={}^{0}\tilde{\boldsymbol{\omega}}_{10}(t)\,{}^{0}\vec{r}_{sm}+{}^{0}\left[{}^{1}\dot{\vec{r}}_{sm}\right] \quad m\in[1,n_S] \tag{2.48} $$

Where:

$ {}^{0}\vec{v}_{sm}(t) $ Velocity vector of each point of the spiral in system O_0 $[\text{m/s}]$

$ {}^{0}\left[{}^{1}\dot{\vec{r}}_{sm}\right] $ Velocity of the points over the spirals in system O_1 transformed into system O_0 $[\text{m/s}]$

$ {}^{0}\vec{\omega}_{10} $ Angular velocity vector of O_1 respect O_0 in system O_0 $[\text{rad/s}]$

Also, derivate the equation (2.7) and multiplying by the transforming matrix form O_1 to O_0, we obtain:

$$ {}^{0}\left[{}^{1}\dot{\vec{r}}_{sm}(t)\right]=\begin{bmatrix} -\dfrac{L\varphi\cos(\varphi)\cos(\theta)\dot{\theta}\dfrac{dC_R(\theta)}{d\theta}}{4\pi}-\dfrac{L\varphi\sin(\varphi)\sin(\theta)\dot{\theta}\dfrac{dC_R(\theta)}{d\theta}}{4\pi} \\ \dfrac{L\varphi\cos(\theta)\sin(\varphi)\sin(\phi)\dot{\theta}\dfrac{dC_R(\theta)}{d\theta}}{4\pi}-\dfrac{L\varphi\cos(\varphi)\sin(\theta)\sin(\phi)\dot{\theta}\dfrac{dC_R(\theta)}{d\theta}}{4\pi} \\ -\dfrac{L\varphi\cos(\theta)\cos(\phi)\sin(\varphi)\dot{\theta}\dfrac{dC_R(\theta)}{d\theta}}{4\pi}+\dfrac{L\varphi\cos(\varphi)\cos(\phi)\sin(\theta)\dot{\theta}\dfrac{dC_R(\theta)}{d\theta}}{4\pi} \end{bmatrix} \tag{2.49} $$

2.6.2 Derivation from O_0 to O_F

From the equation (2.19) we make the following transformation

$$\begin{bmatrix} {}^{F}x_{sm} \\ {}^{F}y_{sm} \\ {}^{F}z_{sm} \end{bmatrix} = \begin{bmatrix} d_x(t) \\ d_y(t) \\ d_z(t) \end{bmatrix} + {}^{F0}\mathbf{T}_Z(t) \begin{bmatrix} {}^{0}x_{sm} \\ {}^{0}y_{sm} \\ {}^{0}z_{sm} \end{bmatrix} \quad m \in [1, n_S] \tag{2.19}$$

Equivalent to

$${}^{F}\vec{R}_{sm}(t) = \vec{r}_{0F}(t) + {}^{F0}\mathbf{T}_Z(t)\ {}^{0}r_{sm}(t) \quad m \in [1, n_S] \tag{2.19}$$

Or

$${}^{F}\vec{R}_{sm}(t) = \vec{r}_{0F}(t) + {}^{F}r_{sm}(t) \quad m \in [1, n_S]$$

Where:

${}^{F}\vec{R}_{sm}(t)$ Position vector of each point of the spiral in system O_F $[\mathrm{m}]$

$\vec{r}_{0F}$ Position vector of the system O_0 respect the system O_F $[\mathrm{m}]$

${}^{F}r_{sm}(t)$ Position vector of each point of the spiral in system O_0 transformed into system O_F $[\mathrm{m}]$

The relative velocity vector between systems is can be direct derivate because it is expressed in the system O_F; but we need to make a new expression for $\Delta\theta$:

$$\Delta\theta = \theta(t) - \theta(t-1) \tag{2.50}$$

The equation is also expressed two times but in different terms in order to notice the new notation, also to simplify the derivation process and the subsequence equation we will obtain, we will work without the matrix $\mathbf{T}_s$ which gives the rotation product of the number of spirals and their distribution; but, first, we need to find expression to determine $\dot{\phi}$ and $\dot{\psi}$ from the geometric changes

- Derivation of $\dot{\phi}$

Also in the apart 2.4.4, the angle χ equal to ϕ numerically, also in the Figure 2-10, this angle is a function of θ, so we can make the following derivate operation:

$$\frac{dC_R\left(\theta(t)\right)}{dt} = \frac{dC_R\left(\theta(t)\right)}{d\theta(t)}\dot{\theta}(t) \tag{2.51}$$

Also

$$\dot{\phi}(t) = \frac{d\chi\left(\theta(t)\right)}{dt} = \frac{d\chi\left(\theta(t)\right)}{d\theta(t)}\dot{\theta}(t) \tag{2.52}$$

Where:

$\dot{\phi}(t)$ Derivate in the time of the angle ϕ $\left[\text{rad/s}\right]$

Also we assume that the conicity has a lineal variation as function of theta, it means:

$$\frac{d^2C_R\left(\theta(t)\right)}{d\theta(t)^2} = 0 \tag{2.53}$$

Consequently:

$$\frac{d^2\chi\left(\theta(t)\right)}{d\theta(t)^2} = 0 \tag{2.54}$$

And also its final and initial value is evaluated using the input data for the segment of the trajectory which is analyzed:

$$\frac{d\,C_R\left(\theta(t)\right)}{d\theta} = \frac{C_{R,f} - C_{R,0}}{\theta_f - \theta_0} \tag{2.55}$$

Where

$C_{R,\mathrm{f}}$ Final value of conicity in the segment

$C_{R,0}$ Initial value of conicity in the segment

In the same way, as we considered the lineal behavior for the conicity angle, we will only calculated the value at the extremes of the interval an the division by the angle will be the value of the

$$\frac{d\chi(\theta(t))}{d\theta} = \frac{\arctan\left(\frac{C_{R,f}}{2}\right) - \arctan\left(\frac{C_{R,0}}{2}\right)}{\theta_f - \theta_0} \tag{2.56}$$

Replacing (2.56) in (2.52):

$$\dot{\phi}(t) = \frac{d\chi(\theta(t))}{dt} = \left(\frac{\arctan\left(\frac{C_{R,f}}{2}\right) - \arctan\left(\frac{C_{R,0}}{2}\right)}{\theta_f - \theta_0} \right) \dot{\theta}(t) \tag{2.57}$$

- Derivation of $\dot{\psi}$

From the equation (2.13) and, also, replacing indeed the equation (2.50) we obtain the following expression:

$$\psi(t) = \psi(t-1) + \frac{r_0\,\theta(t) - \theta(t-1)}{R_K(t)} \tag{2.58}$$

Derivate the equation (2.58):

$$\dot{\psi}(t) = \frac{r_0\,\dot{\theta}(t)}{R_k(t)} - \frac{r_0\,\theta(t)\,\dot{R}_K(t)}{R_k(t)^2} \tag{2.59}$$

Where

$\dot{\psi}(t)$ Derivate in the time of the angle ψ [rad/s]

From the definition of the R_K in the equation (2.8) :

$$\dot{R}_K(t) = \frac{d\,\frac{r_0}{\sin(\chi(\theta(t)))}}{dt} = \frac{2\cos(\chi(\theta(t)))\,r_0\dot{\theta}(t)\,\frac{d\chi(\theta(t))}{dt}}{-1+\cos(2\chi(\theta(t)))} \tag{2.60}$$

Replacing the equation (2.57) in (2.60)

$$\dot{R}_K(t) = \frac{2r_0\,\dot{\theta}(t)^2\cos\left(\chi\left(\theta(t)\right)\right)}{\cos\left(2\chi\left(\theta(t)\right)\right)-1}\left(\frac{\arctan\left(\frac{C_{R,f}}{2}\right)-\arctan\left(\frac{C_{R,0}}{2}\right)}{\theta_f-\theta_0}\right) \tag{2.61}$$

Introducing (2.61) in (2.59), and using the :

$$\dot{\psi}(t) = \frac{r_0\,\dot{\theta}}{R_k(t)} - \frac{2r_0^2\theta\,\dot{\theta}\cos\left(\chi\left(\theta(t)\right)\right)}{R_k(t)^2\cos\left(2\chi\left(\theta(t)\right)\right)-1}\dot{\phi} \tag{2.62}$$

Using also the relation (2.10) in (2.62):

$$\dot{\psi}(t) = r_0\,\dot{\theta}(t)\left(\frac{1}{R_k(t)} - \frac{2r_0\,\theta(t)\cos\left(\phi(t)\right)}{R_k(t)^2\cos\left(2\phi(t)\right)-1}\dot{\phi}(t)\right) \tag{2.63}$$

The expressions (2.57) and (2.63) will not be replaced in the further matricial equation due that will complicate the expressions unnecessarily; however, these equations must be considered when the algorithm for the calculus is developed as a related variables.

- Calculus of the velocity equations

Calculating the derivate, both sides of (2.19)

$$^F\dot{\vec{R}}_{sm}(t) = \dot{\vec{r}}_{0F}(t) + \frac{d\left(^{F0}\mathbf{T}_Z(t)\;{}^0r_{sm}(t)\right)}{dt} \tag{2.64}$$

$$^F\vec{v}_{sm}(t) = \vec{v}_{0F}(t) + \frac{d\left(^{F0}\mathbf{T}_Z(t)\;{}^0r_{sm}(t)\right)}{dt}$$

Where:

$^F\vec{v}_{sm}(t)$ Velocity vector of each point of the spiral in system O_F $[\text{m/s}]$

$\vec{v}_{0F}(t)$ Velocity vector of the system O_0 respect the system O_F $[\text{m/s}]$

Replacing (2.50) in (2.15) and (2.16); and calculating the derivate of the relative position, we obtain:

$$\vec{v}_{0\mathrm{F}}(t)=\vec{v}_{1\mathrm{F}}(t)=\begin{pmatrix}\cos(\psi)r_0\dot{\theta}-\sin(\psi)r_0\theta\dot{\psi}\\ \sin(\psi)r_0\dot{\theta}+\cos(\psi)r_0\theta\dot{\psi}\\ -\sin(\phi)r_0\dot{\phi}\end{pmatrix} \tag{2.65}$$

Due the system O_0 and O_1 are coincident, and in order to simplify the further derivation process we will change the equation (2.19):

$${}^{F}\vec{r}_{sm}(t)=\vec{r}_{1F}(t)+{}^{\mathrm{F1}}\mathbf{T}(t)\,{}^{1}\vec{r}_{sm}(t)\quad m\in[1,n_S] \tag{2.66}$$

Where

$\vec{v}_{1\mathrm{F}}(t)$ Velocity vector of the system O_1 respect the system O_F $[\mathrm{m/s}]$

Also the transformation matrix between this two system:

$${}^{\mathrm{F1}}\mathbf{T}(t)={}^{F0}\mathbf{T}_Z(t)\,{}^{01}\mathbf{T}(t) \tag{2.67}$$

${}^{\mathrm{F1}}\mathbf{T}(t)$ Transformation matrix from O_F to O_1

We can apply the equation of Poisson to obtain the angular velocity of the system O_1 respect O_F in the system O_F

$${}^{\mathrm{F}}\tilde{\boldsymbol{\omega}}_{1F}(t)={}^{\mathrm{F1}}\dot{\mathbf{T}}(t)\,{}^{\mathrm{F1}}\mathbf{T}^{\mathrm{T}}(t) \tag{2.68}$$

Where:

${}^{\mathrm{F}}\tilde{\boldsymbol{\omega}}_{1\mathrm{F}}(t)$ Angular speed skew symmetric matrix of O_1 respect O_F in system O_F $[\mathrm{rad/s}]$

${}^{\mathrm{F1}}\dot{\mathbf{T}}(t)$ Derivate in the time of the transformation matrix from O_F to O_1

${}^{\mathrm{F0}}\dot{\mathbf{T}}_Z(t)$ Derivate in the time of the transformation matrix from O_F to O_0

Also

$$^{F1}\dot{\mathbf{T}}(t) = {}^{F0}\dot{\mathbf{T}}_Z(t)\,{}^{01}\mathbf{T}(t) + {}^{F0}\mathbf{T}_Z(t)\,{}^{01}\dot{\mathbf{T}}(t) \tag{2.69}$$

And we can apply this property of the tensors:

$$^{F1}\mathbf{T}^{T}(t) = \left({}^{F0}\mathbf{T}_Z(t)\,{}^{01}\mathbf{T}(t)\right)^{T} = {}^{F0}\mathbf{T}_Z^{T}(t)\,{}^{01}\mathbf{T}^{T}(t) \tag{2.70}$$

Replacing (2.70) and (2.69) in (2.68)

$$^{F}\tilde{\boldsymbol{\omega}}_{1F}(t) = {}^{F0}\dot{\mathbf{T}}_Z(t)\,{}^{01}\mathbf{T}(t)\,{}^{01}\mathbf{T}^{T}(t)\,{}^{F0}\mathbf{T}_Z^{T}(t) + {}^{F0}\mathbf{T}_Z(t)\,{}^{01}\dot{\mathbf{T}}(t)\,{}^{01}\mathbf{T}^{T}(t)\,{}^{F0}\mathbf{T}_Z^{T}(t) \tag{2.71}$$

$$^{F}\tilde{\boldsymbol{\omega}}_{1F}(t) = {}^{F}\tilde{\boldsymbol{\omega}}_{0F}(t) + {}^{F0}\mathbf{T}_Z(t)\,{}^{0}\tilde{\boldsymbol{\omega}}_{10}(t)\,{}^{F0}\mathbf{T}_Z^{T}(t) \tag{2.72}$$

There is the following tensor property:

$$^{F}\tilde{\boldsymbol{\omega}}_{10}(t) = {}^{F0}\mathbf{T}_Z(t)\,{}^{0}\tilde{\boldsymbol{\omega}}_{10}(t)\,{}^{F0}\mathbf{T}_Z^{T}(t) \tag{2.73}$$

Replacing (2.73) in (2.72):

$$^{F}\tilde{\boldsymbol{\omega}}_{1F}(t) = {}^{F}\tilde{\boldsymbol{\omega}}_{0F}(t) + {}^{F}\tilde{\boldsymbol{\omega}}_{10}(t) \tag{2.74}$$

Where:

$^{F}\tilde{\boldsymbol{\omega}}_{0F}(t)$ Angular speed skew symmetric matrix of O_0 respect O_F in system O_F $[\text{rad/s}]$

To evaluate $^{F}\tilde{\boldsymbol{\omega}}_{10}(t)$, we use the equations (2.14) and (2.46):

$$^{F}\tilde{\boldsymbol{\omega}}_{10}(t) = \begin{bmatrix} 0 & -\sin(\phi)\dot{\theta} & \cos(\phi)\cos(\psi)\dot{\theta} - \sin(\psi)\dot{\phi} \\ \sin(\phi)\dot{\theta} & 0 & -\cos(\phi)\sin(\psi)\dot{\theta} - \cos(\psi)\dot{\phi} \\ -\cos(\phi)\cos(\psi)\dot{\theta} + \sin(\psi)\dot{\phi} & \cos(\phi)\sin(\psi)\dot{\theta} + \cos(\psi)\dot{\phi} & 0 \end{bmatrix} \tag{2.75}$$

Derivate the equation (2.14) and calculating $^{F}\tilde{\boldsymbol{\omega}}_{0F}(t)$

$$^{F}\tilde{\boldsymbol{\omega}}_{0F}(t) = \begin{bmatrix} 0 & \dot{\psi}(t) & 0 \\ -\dot{\psi}(t) & 0 & 0 \\ 0 & 0 & 0 \end{bmatrix} \tag{2.76}$$

Adding (2.75) and (2.76), we obtain:

$$ {}^{\mathrm{F}}\tilde{\boldsymbol{\omega}}_{1\mathrm{F}}(t)=\begin{bmatrix} 0 & -\sin(\phi)\dot{\theta}+\dot{\psi} & \cos(\phi)\cos(\psi)\dot{\theta}-\sin(\psi)\dot{\phi} \\ \sin(\phi)\dot{\theta}-\dot{\psi} & 0 & -\cos(\phi)\sin(\psi)\dot{\theta}-\cos(\psi)\dot{\phi} \\ -\cos(\phi)\cos(\psi)\dot{\theta}+\sin(\psi)\dot{\phi} & \cos(\phi)\sin(\psi)\dot{\theta}+\cos(\psi)\dot{\phi} & 0 \end{bmatrix} \tag{2.77} $$

This is the angular velocity of the system 1 respect the system attached at the origin of the plane, over the robot rolls.

Finally, the velocity of each point of the spiral is defined by the equations (2.65) and (2.48) in the following equation:

$$ {}^{\mathrm{F}}\vec{v}_R = \vec{v}_{0F}(t) + {}^{\mathrm{F}}\tilde{\boldsymbol{\omega}}_{0\mathrm{F}}(t)\,{}^{F}\vec{r}_{sm}(t) + {}^{\mathrm{F0}}\mathbf{T}_Z^{\mathrm{T}}(t)\,{}^{0}\vec{v}_{sm}(t) \tag{2.78} $$

This last equation expresses the velocity for each point over the spirals at each instant of time. Due the length of this equation it only will be expressed symbolically; however, replacing all the members of its, it can be implemented in a computational calculus software.

2.7 Acceleration Equations

The process used to obtain the velocity equation is repeated in the obtaining of the acceleration equation, we will derive the equation from O_0 to O_1 and from O_F to O_0; but, it is necessary to derivate $\ddot{\phi}$ and $\ddot{\psi}$:

- Derivation of $\ddot{\phi}$

From the equation (2.52) we obtain a second derivate of ϕ:

$$ \frac{d^2\chi(\theta(t))}{dt^2} = \frac{d\chi(\theta(t))}{dt}\ddot{\theta} + \left(\frac{d\chi(\theta(t))}{dt}\right)^2 \frac{d^2\chi(\theta(t))}{d\theta(t)^2} \tag{2.79} $$

Replacing (2.54) and (2.57)

$$ \ddot{\phi} = \left(\frac{\arctan\left(\frac{C_{R,f}}{2}\right) - \arctan\left(\frac{C_{R,0}}{2}\right)}{\theta_f - \theta_0} \right) \dot{\theta}\ddot{\theta} \tag{2.80} $$

- Derivation of $\ddot{\psi}$

From the equation (2.59):

$$\ddot{\psi}(t) = -\frac{2r_0\,\dot{\theta}\dot{R}_K(t)}{R_K(t)^2} + \frac{2r_0\,\theta\dot{R}_K(t)^2}{R_K(t)^3} + \frac{r_0\,\ddot{\theta}}{R_K(t)} - \frac{r_0\theta\ddot{R}_k(t)}{R_K(t)^2} \tag{2.81}$$

To obtain $\ddot{R}_K$, we derive the equation (2.60) and simplifying:

$$\ddot{R}_K(t) = \frac{r_0}{\sin(\phi)}\left(\frac{-\frac{d\chi(\theta)}{d\theta}\ddot{\theta}}{\tan(\phi)} + \dot{\theta}^2\left(\left(\frac{d\chi(\theta)}{d\theta}\right)^2\left(\frac{1}{\tan(\phi)^2} + \frac{1}{\sin(\phi)^2}\right)\right)\right) \tag{2.82}$$

2.7.1 Derivation from O_1 to O_0

The expression (2.48) can be directed derivate to obtain the expression of the acceleration between these two systems:

$${}^0\vec{a}_{sm}(t) = {}^0\tilde{\boldsymbol{\alpha}}_{10}(t)\,{}^0\vec{r}_{sm}(t) + {}^0\tilde{\boldsymbol{\omega}}_{10}(t)\,{}^0\tilde{\boldsymbol{\omega}}_{10}(t)\,{}^0\vec{r}_{sm}(t) + 2\,{}^0\tilde{\boldsymbol{\omega}}_{10}(t)\,{}^0\left[{}^1\dot{\vec{r}}_{sm}\right] + {}^0\left[{}^1\ddot{\vec{r}}_{sm}\right] \quad m \in [1, n_S] \tag{2.83}$$

Where:

${}^0\vec{a}_{sm}(t)$	Acceleration vector of each point of the spiral in system O_0 $\left[\text{m/s}^2\right]$
${}^0\tilde{\boldsymbol{\alpha}}_{10}(t)$	Angular acceleration skew symmetric matrix of O_1 respect O_0 in system O_0 $\left[\text{rad/s}^2\right]$
${}^0\left[{}^1\ddot{\vec{r}}_{sm}\right]$	Acceleration of the points over the spirals in system O_1 transformed into system O_0 $\left[\text{m/s}^2\right]$

The angular acceleration of O_1 from O_0 in system O_0 is directly derivate from (2.46):

$$ {}^{0}\tilde{\boldsymbol{\alpha}}_{10}(t)=\begin{bmatrix} 0 & -\cos(\phi)\dot{\theta}\dot{\phi}-\sin(\phi)\ddot{\theta} & -\sin(\phi)\dot{\theta}\dot{\phi}+\cos(\phi)\ddot{\theta} \\ \cos(\phi)\dot{\theta}\dot{\phi}+\sin(\phi)\ddot{\theta} & 0 & -\ddot{\phi} \\ \sin(\phi)\dot{\theta}\dot{\phi}-\cos(\phi)\ddot{\theta} & \ddot{\phi} & 0 \end{bmatrix} \tag{2.84} $$

Additionally, the expression for ${}^{0}\left[{}^{1}\ddot{\vec{r}}_{sm}\right]$ is showed reduced:

$$ {}^{0}\left[{}^{1}\ddot{\vec{r}}_{sm}\right]=\begin{bmatrix} -\dfrac{L\varphi\cos(\varphi)\cos(\theta)\ddot{\theta}\dfrac{dC_R(\theta)}{d\theta}}{4\pi}-\dfrac{L\varphi\sin(\varphi)\sin(\theta)\ddot{\theta}\dfrac{dC_R(\theta)}{d\theta}}{4\pi} \\ \dfrac{L\varphi\cos(\theta)\sin(\varphi)\sin(\phi)\ddot{\theta}\dfrac{dC_R(\theta)}{d\theta}}{4\pi}-\dfrac{L\varphi\cos(\varphi)\sin(\theta)\sin(\phi)\ddot{\theta}\dfrac{dC_R(\theta)}{d\theta}}{4\pi} \\ -\dfrac{L\varphi\cos(\theta)\cos(\phi)\sin(\varphi)\ddot{\theta}\dfrac{dC_R(\theta)}{d\theta}}{4\pi}+\dfrac{L\varphi\cos(\varphi)\cos(\phi)\sin(\theta)\ddot{\theta}\dfrac{dC_R(\theta)}{d\theta}}{4\pi} \end{bmatrix} \tag{2.85} $$

The equation (2.83) is showed symbolically due to its length

2.7.2 Derivation from O_0 to O_F

The equation (2.78) will be directed derivate to obtain the acceleration:

$$ {}^{F}\vec{a}_{sm}=\vec{a}_{0F}(t)+{}^{F}\tilde{\boldsymbol{\alpha}}_{0F}(t)\,{}^{F}\vec{r}_{sm}(t)+{}^{F}\tilde{\boldsymbol{\omega}}_{0F}(t)\,{}^{F}\tilde{\boldsymbol{\omega}}_{0F}(t)\,{}^{F}\vec{r}_{sm}(t)+{}^{F0}\mathbf{T}_{Z}^{T}(t)\,{}^{0}\vec{a}_{sm}(t)+2\,{}^{F}\tilde{\boldsymbol{\omega}}_{0F}(t)\,{}^{F}\left[{}^{0}\vec{v}_{sm}(t)\right] \tag{2.86} $$

Where:

- ${}^{F}\vec{a}_{sm}(t)$ — Acceleration vector of each point of the spiral in system O_F $\left[\text{m/s}^2\right]$
- ${}^{F}\tilde{\boldsymbol{\alpha}}_{0F}(t)$ — Angular acceleration skew symmetric matrix of O_0 respect O_F in system O_F $\left[\text{rad/s}^2\right]$
- $\vec{a}_{0F}(t)$ — Acceleration vector of the system O_0 respect the system O_F $\left[\text{m/s}^2\right]$

The acceleration of the system O_0 respect O_F is directed derivate from the equation (2.76):

$$ {}^{F}\tilde{\boldsymbol{\alpha}}_{0F}(t) = \begin{bmatrix} 0 & \ddot{\psi}(t) & 0 \\ -\ddot{\psi}(t) & 0 & 0 \\ 0 & 0 & 0 \end{bmatrix} \tag{2.87} $$

Finally the acceleration the system O_0 respect the system O_F :

$$ \vec{a}_{0F}(t) = \begin{bmatrix} -2r_0 \sin\psi\dot{\theta}\dot{\psi} - \theta\dot{\psi}^2 r_0 \cos\psi + \ddot{\theta} r_0 \cos\psi - \theta\ddot{\psi} r_0 \sin\psi \\ 2r_0 \cos\psi\dot{\theta}\dot{\psi} - \theta\dot{\psi}^2 r_0 \sin\psi + \ddot{\theta} r_0 \sin\psi + \theta\ddot{\psi} r_0 \cos\psi \\ -\dot{\phi}^2 r_0 \cos\phi - \ddot{\phi} r_0 \sin\phi \end{bmatrix} \tag{2.88} $$

To close this chapter, all the expression showed here are necessary to analyze and control the movement of the robot. The following chapter will offer a briefly summaries for some algorithm and ideas to the performing of these movements and geometrical changes.

(Next) Section 1

CHAPTER 3 ROBOT ROLLING MOVEMENT CONTROL STRATEGIES

3.1 Introduction

Within the robot, there are only two kinematic independent variables, the conicity angle or roll angle ϕ, which is performed by the geometrical change of the robot and, in consequence, the movement angle ψ is developed.

The pitch angle θ is performed by the rolling movement of the robot, about the generation of this angle and its control will treat this chapter. The physical principle, which this movement is generated, is the unbalanced torque around the y_0 axis of the robot; also technological alternatives will be proposed in this chapter.

3.2 Movement Impulse – Traveling Masses over a Spiral

We will suppose there is only a spiral over which a punctual mass is traveling, also the movements of this mass are able to be controlled. If we reply this mass and its spiral many times, we will have built a system in which, the condition the torque exerted around y_0 of the robot depends of the positions of all the mases and the value of the angle θ. This idea is depicted in the following figure:

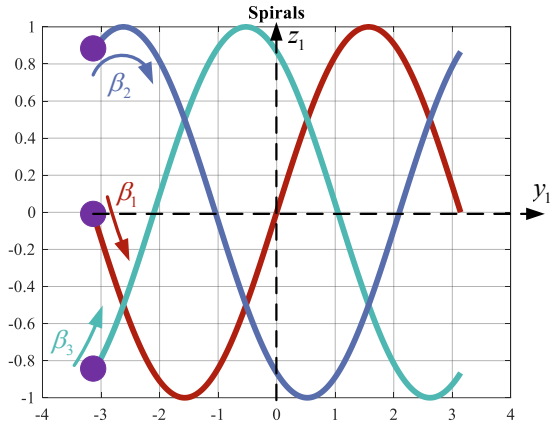

Figure 3-1 Masses over the spirals and their positions angles

Where:

$$\beta_m \qquad \text{Position angle of the impulsive m} - \text{mass} \quad [\text{rad}]$$

The value of β_m comes from $-\pi$ to π, this angle is measured for each spiral when this is not rotated; even, we can define the position of each mass in the system O_1 using the equations (2.1) and (2.3), only changing the angle φ for the angle β_m.

We will suppose that the number of impulsive masses is equal as the number of external spirals; additionally, due to the complex deformation the robot supports, all the impulsive masses are not traveling over the external spiral, also a rigid internal core is proposed, around which these masses will travel. The principal reason to develop this core is the caring of the mechanism which moves and controls the position of the masses; large deformations as the external spirals suffer, might damage or produce malfunctions in the mechanism of the robot.

Therefore, we will suppose there is an internal basis radius for these spirals and, in consequence, it defines the position of the impulsive masses. We rewrite the equations as follow:

$$\vec{r}_{Im} = \begin{bmatrix} r_{0i}\cos(\beta_m) \\ \dfrac{L\beta_m}{\pi} - \dfrac{L}{2} \\ r_{0i}\sin(\beta_m) \end{bmatrix} \quad \beta_m \in [-\pi;\ \pi] \tag{3.1}$$

Where:

$\vec{r}_{Im}$ Position vector of the impulsive m – mass over its spiral $[\mathrm{m}]$

r_{0i} Internal basis radius for the traveling spirals of the impulsive masses $[\mathrm{m}]$

As the case of the external spirals, these internal spirals also are distributed around a circle of radius r_{0i} and also could have an initial rotation similar as it is expressed in the equation (2.3). For simplifying reason we will assume these angles equal as the used for the external spirals:

$$ {}^{1}\vec{r}_{Im} = \begin{bmatrix} {}^{1}x_{\mathrm{Im}} \\ {}^{1}y_{\mathrm{Im}} \\ {}^{1}z_{\mathrm{Im}} \end{bmatrix} = \begin{bmatrix} \cos\left(\varphi_0 + \vartheta(m-1)\right) & 0 & -\sin\left(\varphi_0 + \vartheta(m-1)\right) \\ 0 & 1 & 0 \\ \sin\left(\varphi_0 + \vartheta(m-1)\right) & 0 & \cos\left(\varphi_0 + \vartheta(m-1)\right) \end{bmatrix} \vec{r}_{Im} \tag{3.2} $$

Where:

${}^{1}x_{\mathrm{Im}}, {}^{1}y_{\mathrm{Im}}, {}^{1}z_{\mathrm{Im}}$ Coordinates of the impulsive m – mass in system O_1 $[\mathrm{m}]$

${}^{1}\vec{r}_{Im}$ Position vector of the impulsive m – mass in system O_1 $[\mathrm{m}]$

If we observe the masses in the plane $x_1 - z_1$, as it is depicted in the following figure, we will determine easily the exerted moment around the y_1 axis, which is determined by the weight force multiplied by the position over the x_1 axis. This system has been chosen because this system is turned by the angles $\phi(t)$ and $\theta(t)$; therefore, the kinematic equations must be calculated around this axis.

For the special case when $\phi = 0$ and it remains always in that way, the torque around y_1 is directly calculated by the multiplication of the weight force and its distance to the rotation axis; otherwise, when this system is oriented in different way, when $\phi \neq 0$, the calculation form is different and it will treated in further works. The position system showed in the following figure is valid for both cases:

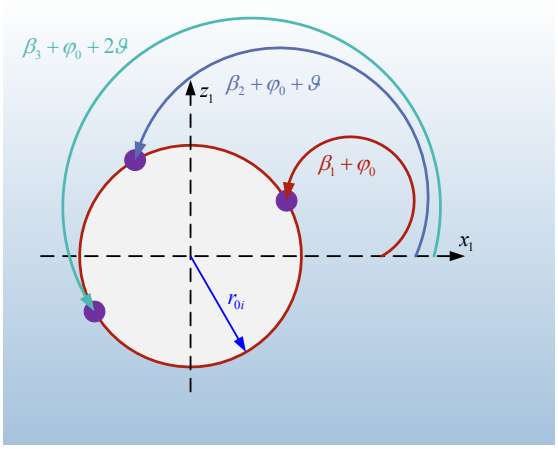

Figure 3-2 Position angles of the impulsive masses in system O_1

The previous figure shows the position angle in the impulsive masses, also due to the rotation around y_1, the final expression which give us the position vector is the resulting product of the equation (3.2) and (2.9):

$$ {}^{1}\vec{r}_{Im} = \begin{bmatrix} \cos\left(\varphi_0 + \vartheta(m-1) + \beta_m(t) + \theta(t)\right) \\ \dfrac{L\beta_m}{\pi} - \dfrac{L}{2} \\ \sin\left(\varphi_0 + \vartheta(m-1) + \beta_m(t) + \theta(t)\right) \end{bmatrix} \tag{3.3} $$

This physic principle is a proposal for the generation of the rolling movement of the robot. The key of the control technics is the variation of the angle β_m which is an independent variable for each mass, and the way to find the best position to produce the desired effect is the focus further in this chapter.

Without considering the kinematic effects of the accelerations to which the system O_1 is subjected, we cannot build a differential equation to calculate the value of θ at each instant of time; although, we can calculate the torque around y_1 transforming the weight vector force of each mass to the system O_1, considering only that the only transformation which affect the system O_1 is the rotation around x_0 given by the equation (2.11):

$$ {}^{1}\vec{F}_{Wm} = \begin{bmatrix} 1 & 0 & 0 \\ 0 & \cos(\phi) & -\sin(\phi) \\ 0 & \sin(\phi) & \cos(\phi) \end{bmatrix} \begin{bmatrix} 0 \\ 0 \\ -m_{\mathrm{Im}} g \end{bmatrix} = \begin{bmatrix} 0 \\ m_{\mathrm{Im}} g \sin(\phi) \\ -m_{\mathrm{Im}} g \cos(\phi) \end{bmatrix} \tag{3.4} $$

Where:

${}^{1}\vec{F}_{Wm}$	Force exerted by the m – mass in system O_1 $\left[\mathrm{N}\right]$
m_{Im}	Mass of the impulsive m – mass $\left[\mathrm{kg}\right]$
g	Gravity acceleration $\left[\mathrm{m/s^2}\right]$

Finally the torque around O_1 exerted by ${}^{1}F_{Wm}$ is given by the following equation:

$$ {}^{1}\vec{T} = {}^{1}\vec{r}_{Im} \times {}^{1}\vec{F}_{Wm} \tag{3.5} $$

Where:

${}^{1}\vec{T}$	Torque in system O_1 $\left[\mathrm{N \cdot m}\right]$

3.3 Technologies for Masses Movement

In this section, some constructive alternatives will be presented in order to obtain a system of masses which can be controlled and moved as according with the needing of the system in order to arrive to a desired value of produced torque or keep a constant value of angular velocity for the rolling $\dot{\theta}$.

3.3.1 Internal Gear Displacement

According with this concept, the internal path of the internal spirals has gear profile acting as a ring gear and the impulsive masses are planet gear which travels around the curved profile of the internal spiral. This idea was developed in [8] and also the following figure was taken for that work:

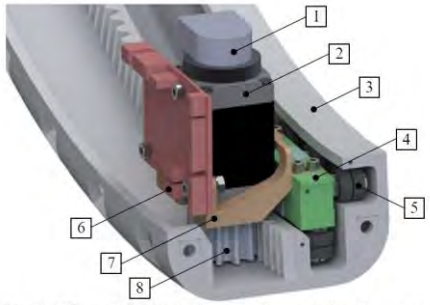

Fig. 6: CAD model with basic parts: 1 – encoder, 2 – stepper motor, 3 – curved member with guide and gear rack, 4 – slide, 5 – ball bearings, 6 – motor controller, 7 – motor mount, 8 – bevel gear wheel.

Figure 3-3 Mechanism for the internal gear displacement. Source: [8]

The principal advantage for this mechanism is the capability to control the position of the masses, which allow us to implement a control algorithm basis on the analysis of several options. The principal disadvantage of this mechanism is the possibility to be blocked by dirtiness or some bigger particles, also by the friction present between gears, some lubrication may be required, therefore a cover should be implemented.

3.4 Strategies for Masses Movement Control

3.4.1 Prediction for Option Analysis

This strategy is based in the combination analysis, where there are a several number of possibilities for movement of the impulsive masses. Each mass, at each interval of time, has the capability to be displaced a determined angle or value of β_m; moreover, this angle could be positive, negative or zero.

Owing to these three possibilities for each mass, the number of different results is given by the following formula:

$$n_P = 3^{n_s} \tag{3.6}$$

An example case, for $n_s = 4$ is showed in the following figure:

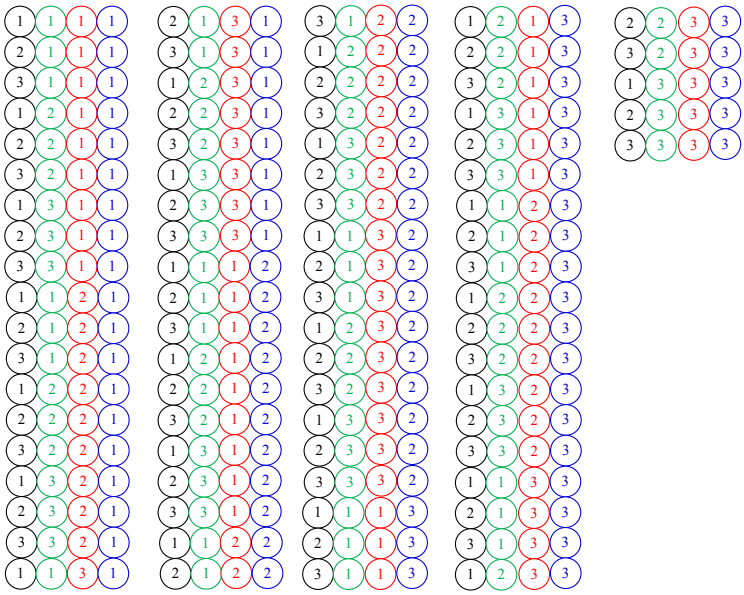

Figure 3-4 Possible cases for $n_s = 4$

Also, not all the cases showed on the previous figure are possibly. An elimination process must be established to determine which cases are impossible due to the masses would be out of the spiral.

In the following equation, an elimination criterion is expressed:

$$\beta_m(t) = \begin{cases} \beta_m(t-1) + \beta_{Pm} < -\pi & \text{Impossible} \\ -\pi \le \beta_m(t-1) + \beta_{Pm} \le \pi & \text{Possible} \\ \beta_m(t-1) + \beta_{Pm} > \pi & \text{Impossible} \end{cases} \tag{3.7}$$

Where:

β_{Pm} Possible incremental value of β_m for the impulsive m – mass $[\text{rad}]$

Once the impossible cases are eliminated from all the cases, we have to choose which of them is close to the desired value of torque around y_1 which is the symmetry axis.

The following figures shows the results of this algorithm for $n_s = 3$ and $r_{0i} = 0,2$ m. For this simulation, we have taken a constant value of $\phi = 0$, it means, y_0 is parallel and

coincident with y_1 and the masses have a weight of $0{,}1\,\text{kg}$. The objective torque to reach is $0\ \text{N}\cdot\text{m}$

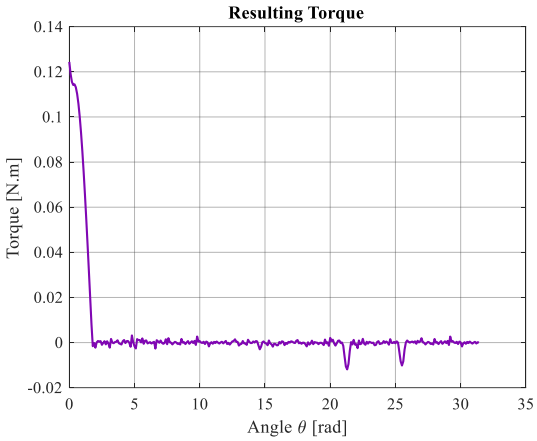

Figure 3-5 Resulting torque through the prediction algorithm of option analysis

To obtain this result, the step of β_{Pm} was 0,05 rad; this value can be added or subtracted, but this is not a function of time, but else it is a function of θ. So, for each increment of θ, the value of $\beta(t)$ is modified. The derivatives of $\beta(t)$ respect the time are limited by the capabilities of the mechanism for masses movement. For this reason, we only will work with an stable increment of β.

Finally, the position of the masses over its spirals along the displacement from we have obtained the previous figure, is depicted in the following image:

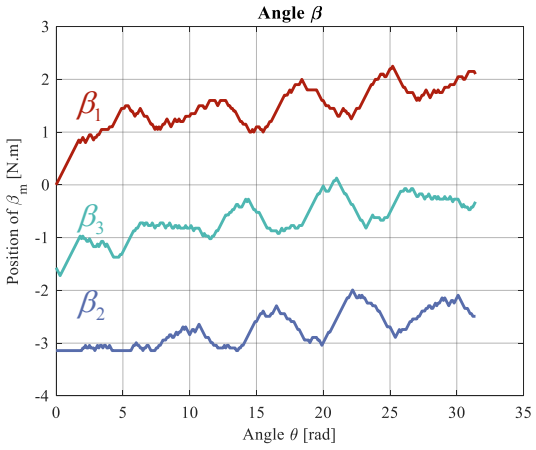

Figure 3-6 Position angles of the impulsive masses

3.4.2 Minimum Distance to the Desired Position

This algorithm is basis on the Lagrange multipliers and it works moving the impulsive masses to the position which is more close to the desired value of torque.

Neglecting the influence of the inclination of the y_1 axis, we depend on the value of the distant given by the coordinate x_1 of the impulsive masses, this coordinate is mathematically a function cosine. So we can express the torque as a sum of cosines as follow:

$$g\left(\Phi_1,\Phi_2,\Phi_3,\mathrm{L}\ ,\Phi_{n_s}\right)=\cos\left(\Phi_1\right)+\cos\left(\Phi_2\right)+\cos\left(\Phi_3\right)+\mathrm{L}\ \cos\left(\Phi_{n_s}\right)={}^1T_y \tag{3.8}$$

For $n_s=3$ in order to obtain a tridimensional surface:

$$g\left(\Phi_1,\Phi_2,\Phi_3\right)=\cos\left(\Phi_1\right)+\cos\left(\Phi_2\right)+\cos\left(\Phi_3\right)=\frac{{}^1T_y}{m_{\mathrm{Im}}g}$$

Also:

$$\Phi_m=\varphi_0+\vartheta\left(m-1\right)+\beta_m\left(t\right)+\theta\left(t\right) \tag{3.9}$$

Where:

${}^1T_y$ Torque exerted around y_1 $\left[\mathrm{N}\cdot\mathrm{m}\right]$

Φ_m Value of the angle turned by the impulsive mass $\left[\mathrm{rad}\right]$

If we see the values of the angles as a coordinates in the spaces, these three angles defines a point in the space.

$$\left(x_P,y_P,z_P\right)=\left(\Phi_1\quad\Phi_2\quad\Phi_3\right)$$

As it is expressed in the equation (3.8), the desired value of torque is given by a similar expression:

$$f\left(\Phi_{1P},\Phi_{2P},\Phi_{3P}\right)=\cos\left(\Phi_{1P}\right)+\cos\left(\Phi_{2P}\right)+\cos\left(\Phi_{3P}\right)=\frac{T_D}{m_{\mathrm{Im}}g} \tag{3.10}$$

Φ_{mP} Objective angle to reach by the impulsive masses $\left[\mathrm{rad}\right]$

T_D Torque to reach by the system $[\mathrm{N}\cdot\mathrm{m}]$

From the equation (3.10) we can define a surface which is the possible solutions to reach the desired torque. So, this can be expressed:

$$\Phi_{3P} = \arccos\left(-\cos(\Phi_{1P}) - \cos(\Phi_{2P}) - \frac{T_D}{m_{\mathrm{Im}} g}\right) \tag{3.11}$$

This surface for $T_D = 0$ is showed in the following figure:

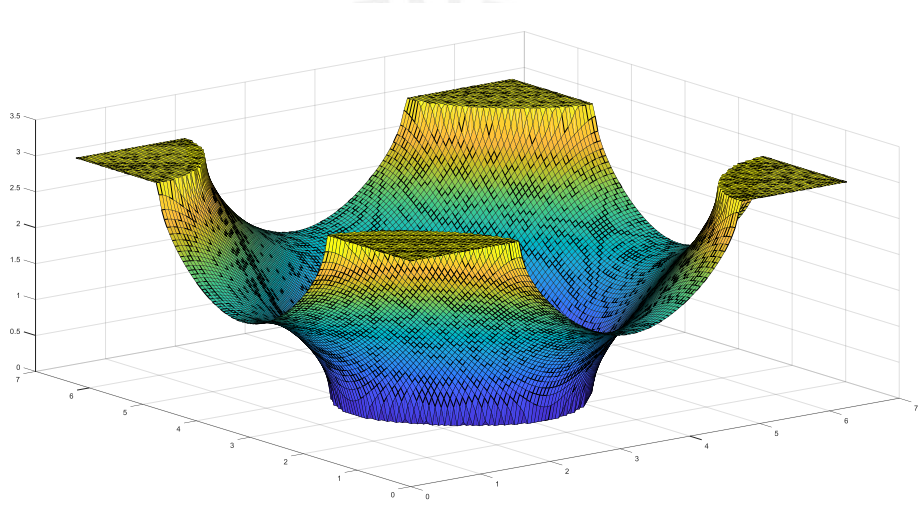

Figure 3-7 Surface of solutions

Due to the domain that the function arc cosine has, there are zones where there is any solution.

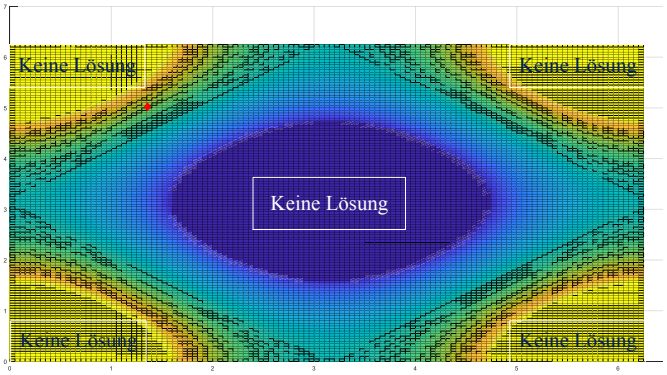

Figure 3-8 Solution areas

The objective of this algorithm is finding the minimum distance between the point given by $(x_P, y_P, z_P) = (\Phi_1 \quad \Phi_2 \quad \Phi_3)$ and the solution surface. This optimization calculus is performed using the Lagrange multipliers:

$$\mathcal{L}(\Phi_{1P}, \Phi_{2P}, \Phi_{3P}, \lambda) = \sqrt{(-\Phi_1 + \Phi_{1P})^2 + (-\Phi_2 + \Phi_{2P})^2 + (-\Phi_3 + \Phi_{3P})^2} - \lambda(\cos(\Phi_{1P}) + \cos(\Phi_{2P}) + \cos(\Phi_{3P}) - 0) \quad (3.12)$$

The non-lineal system to be solved is the gradient of the lagrangian function expressed in the following equation:

$$\nabla\mathcal{L} = \begin{Bmatrix} \dfrac{-\Phi_1 + \Phi_{1P}}{\sqrt{(-\Phi_1 + \Phi_{1P})^2 + (-\Phi_2 + \Phi_{2P})^2 + (-\Phi_3 + \Phi_{3P})^2}} + \lambda \sin(\Phi_{1P}) \\ \dfrac{-\Phi_2 + \Phi_{2P}}{\sqrt{(-\Phi_1 + \Phi_{1P})^2 + (-\Phi_2 + \Phi_{2P})^2 + (-\Phi_3 + \Phi_{3P})^2}} + \lambda \sin(\Phi_{2P}) \\ \dfrac{-\Phi_3 + \Phi_{3P}}{\sqrt{(-\Phi_1 + \Phi_{1P})^2 + (-\Phi_2 + \Phi_{2P})^2 + (-\Phi_3 + \Phi_{3P})^2}} + \lambda \sin(\Phi_{3P}) \\ -\cos(\Phi_{1P}) - \cos(\Phi_{2P}) - \cos(\Phi_{3P}) \end{Bmatrix} = \begin{Bmatrix} 0 \\ 0 \\ 0 \\ 0 \end{Bmatrix} \quad (3.13)$$

The solutions of this system are the values of $(\Phi_{1P}, \Phi_{2P}, \Phi_{3P})$ and λ which gives the minimum distance from the point to the solution surface. Finally the new values of β_m are determined by the different between the results and $(x_P, y_P, z_P) = (\Phi_1 \quad \Phi_2 \quad \Phi_3)$.

(next) Section

CHAPTER 4 GEOMETRY VARIATIONS

4.1 Introduction

The transformation from cylindrical to conical shape implies large deformations along the compressed member of the tensegrity robot, the forces which perform such deformations must be located in that way that the principal effect should be the radial displacement of the nodes over the spirals. Also, the material plays and important paper over the capability of the robot to change its geometry without affecting its rolling movement capability. In this chapter, some composite materials are proposed to be used for the spirals; additionally, a basis of procedure of calculus of the internal forces produced by radial forces is presented and a modification of the theory presented in chapter 1 for its application in cylindrical bodies.

4.2 Materials for the Spirals

The main idea to use composite material is taking advantage of the large deformation that some polymer can support and the tensile properties of the fibers in order to avoid the excessive longitudinal deformations.

The following figure shows the orientation searched for the composed material for the spirals:

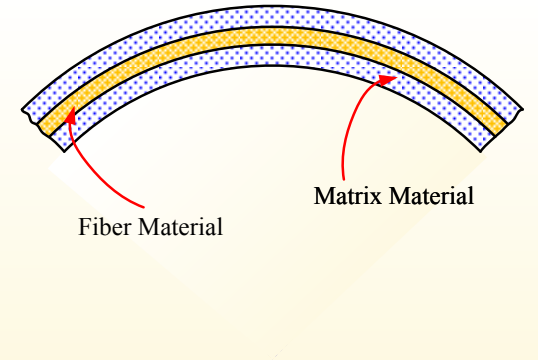

Figure 4-1 Structure of the composed material for the spirals

The elastic modulus on the radial and tangential direction, due to the orientation of the fiber is given by the following relations:

Tangential:

$$E_{tc} = E_f V_f + E_m V_m \tag{4.1}$$

Where:

E_{tc} Elastic modulus on the tangential direction of the composite material $\left[\text{N/mm}^2\right]$

E_f Elastic modulus of the fiber material $\left[\text{N/mm}^2\right]$

E_m Elastic modulus of the matrix material $\left[\text{N/mm}^2\right]$

V_f Volume fraction of the fiber material over the total volume

V_m Volume fraction of the matrix material over the total volume

Radial:

$$\frac{1}{E_{rc}} = \frac{V_f}{E_f} + \frac{V_m}{E_m} \tag{4.2}$$

Where:

E_{rc} Elastic modulus on the radial direction of the composite material $\left[\mathrm{N/mm^2}\right]$

This kind of material presents a highest anisotropic behavior, due to this characteristic, is important notice that each direction will show different deformation when they are subjected to the same load. Following, an alternative of composite material are presented.

4.2.1 Kevlar® Fiber and Elastomer Matrix

The mechanical properties of each of them are presented in the following table:

Table 4-1 Mechanical properties of Kevlar and Rubber Source: [16]

Material	Density ρ $\left[\mathrm{kg/m^3}\right]$	Tensile strength σ_B $\left[\mathrm{MPa}\right]$	Elongation at failure %	Elastic Modulus $\left[\mathrm{GPa}\right]$
Kevlar	1450	134	3.5	120
Polyisoprene	930	20,68	800	0.02
Butadiene - Styrene	1000	20,68	400	0.03

Additionally, it must be considered that the elasticity modulus for this polymers have changes depending on the orientation of the applied load. For the scopes of this work, only we present the results of the elasticity modulus according to the equations (4.1) and (4.2) for different values of volume fraction of fiber material.

The following figure shows the set of values for a range from 10% to 70% of volume fraction of fiber material (Kevlar) on the radial and tangential direction. Further, in this chapter, we only will refer in, a symbolic way, to these mechanical properties, leaving the optimization of this material to a future works.

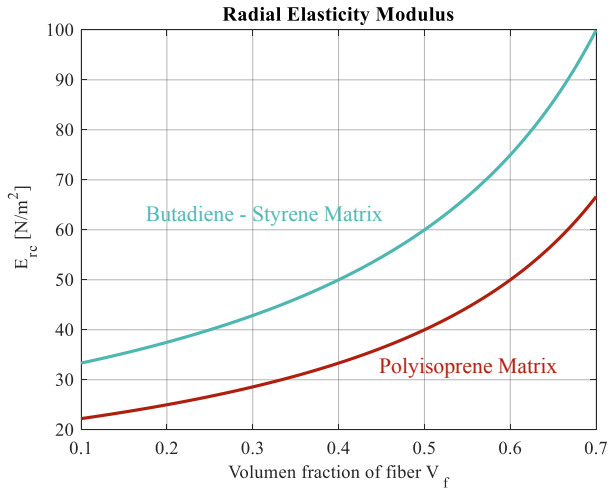

Figure 4-2 Radial elastic modulus for different matrix material

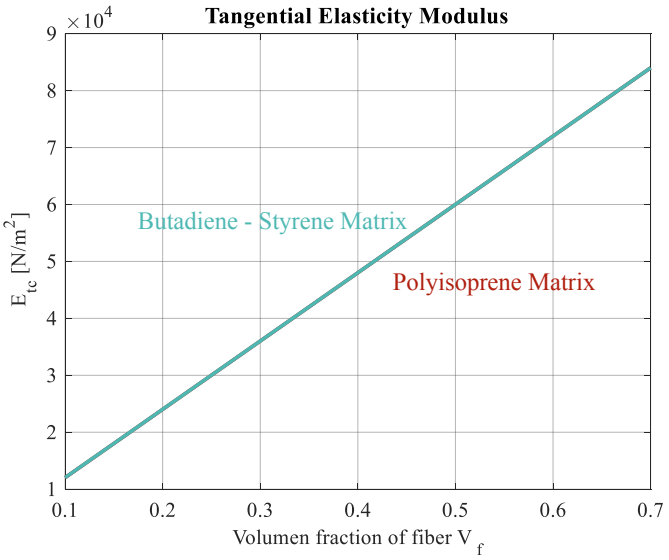

Figure 4-3 Tangential elastic modulus for different matrix material

The principal influence is viewed in the radial elastic modulus; however, over the tangential elastic modulus, the matrix material has any effect.

4.3 Tensegrity Description for Rotational Geometries

All the concepts explained in the chapter 1, could be reoriented using another coordinate system. This is, also, based on the same principles, but with the difference that this concept should be transformed into a cylindrical coordinate system.

In the specific case of this robot, there is a spiral geometry given by the equation (2.7) and also rotated and distributed around the y_1 axis. In the next subchapter, the process to determine the best configuration is presented.

4.3.1 Transformation of the matrix of nodes

The vector of nodes $\vec{n}$ and the matrix of nodes are expressed in Cartesian coordinates; therefore, the transformation must be made considering which is the longitudinal coordinate and which are the transversal coordinates; it is given using the following relations for robot focus of this work:

$$\mathbf{N}_\theta = \begin{bmatrix} r_{Sn} \\ \theta_{Sn} \\ l_{Sn} \end{bmatrix} = \begin{bmatrix} \sqrt{x_1^2 + z_1^2} & \cdots & \sqrt{x_n^2 + z_n^2} \\ \arctan\left(\frac{z_1}{x_1}\right) & \cdots & \arctan\left(\frac{z_n}{x_n}\right) \\ y_1 & \cdots & y_n \end{bmatrix} \tag{4.3}$$

Where:

$\mathbf{N}_\theta$	Matrix of nodes expressed in cylindrical coordinates
r_{Sn}	Radial coordinate of a node
θ_{Sn}	Angular coordinate of a node
l_{Sn}	Polar longitudinal coordinate of a node

The matrix of nodes could be expressed, also, in conical coordinates, but owing to the complicated expressions and the fact that the system can be expressed in cylindrical system, this idea was not considered for the present work. In the other hand, the transformation and expression of in that system could be used in further applications.

4.3.2 Transformation of the Matrix of element

The matrix of elements can be expressed in the same way, as it is expressed for Cartesian coordinates, as a difference of the node coordinates of the nodes which composed the element, but with the differences that there is a relation between θ_S and r_S ,it means that r_S is a function of θ_S ; this idea will be used further to determine the length of the elements. This relation, for the conical case, is a lineal correspondence. The matrix of elements is expressed as follow:

$$\mathbf{M}_\theta = \begin{bmatrix} r_{Sm} \\ \theta_{Sm} \\ l_{Sm} \end{bmatrix} = \begin{bmatrix} r_{S11} - r_{S10} & \cdots & r_{Sm1} - r_{Sm0} \\ \theta_{S11} - \theta_{S10} & \cdots & \theta_{Sm1} - \theta_{Sm0} \\ l_{S11} - l_{S10} & \cdots & l_{Sm1} - l_{Sm0} \end{bmatrix} \tag{4.4}$$

$\mathbf{M}_\theta$ Matrix of elements expressed in cylindrical coordinates

r_{Sm} Radial coordinate of a member

θ_{Sm} Angular coordinate of a member

l_{Sm} Longitudinal coordinate of a member

The subindices 1 and 0 indicate the final node and the initial node respectively. Using the same idea, we can obtain the connectivity matrix for this coordinate system in the same way as the used for Cartesian coordinates. This expression is equal as the equation (1.4), only with the differences that a subindices is used to express that the connection matrix correspond a cylindrical system:

$$\mathbf{M}_\theta = \mathbf{N}_\theta \mathbf{C}_\theta^{\mathrm{T}} \tag{4.5}$$

$\mathbf{C}_\theta^{\mathrm{T}}$ Connectivity matrix in cylindrical coordinates

4.3.3 Matrix of length

As it is expressed before, r_S is a function of θ_S, due to the conical shape that the robot could be adopted, there is a lineal correspondence between this coordinates, so we can express in an interval the following relation:

$$r_S(\theta_S) = r_{Sm0} + \frac{r_{Sm1} - r_{Sm0}}{\theta_{Sm1} - \theta_{Sm0}}(\theta_S - \theta_{Sm0}) \tag{4.6}$$

Also the length of each element expressed in this coordinate system is given as follow

$$L_{\theta m} = \int_{\theta_{Sm0}}^{\theta_{Sm1}} \sqrt{\left(\frac{dl_S}{d\theta}\right)^2 + (r_S)^2 + \left(\frac{dr_S}{d\theta}\right)^2}\, d\theta \tag{4.7}$$

Where

$L_{\theta m}$ Length of a member

4.3.4 Loads in curved elements

A curved member is subjected, mainly, to compression forces and bending moments. In the following figure, we can visualize the case of this load in a cylindrical element:

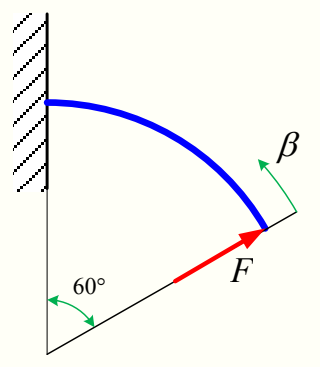

Figure 4-4 Example case of curved element

For a generic angle θ_{Sm} we have the following free body diagram:

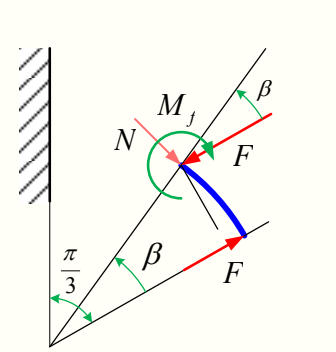

Figure 4-5 Free body diagram for a generic section at generic angle value

From the free body diagram, we obtain the forces over each direction:

$$F_R = F\cos\theta_S \tag{4.8}$$

$$F_T = F\sin\theta_S \tag{4.9}$$

Also the bending moment around the longitudinal symmetrical axis:

$$M_l = FR\sin\theta_S \tag{4.10}$$

Due there is an internal moment along the element, it is impossible to define a density force, instead an energy density must be determined to calculated the equilibrium of the structure. Also, from these equations applied for the geometry, we can determine the total energy produced by flection, and compression. A further evaluation using elasticity theory or finite elements will give the final results for the deformation for different points of load application.

The loads applied over the spiral are exerted by the tensile elements; these elements are pre stressed in order to keep the structure of the spiral together during its working and performing the deformation for the geometrical changes.

FUTURE WORKS AND RECOMMENDATIONS

- Some new techniques for the moving of the impulsive masses should be developed, in order to get a better control and fast moving of these masses to the desired position over the inner spirals.
- A kinetic analysis is required for the knowing of the inertial forces and torques produced by the accelerations.
- From a kinetic analysis, control algorithm should be developed to implement the control system of the robot
- A specialized study in materials is highly required in order to determine the best material configuration for the spirals which are subjected to large deformation.
- A further developing of equilibrium and stability equation must be developed using another coordinates system in order to find the best way to describe the different geometries finding in the spirals. This work, also open the possibility to develop a new way to see the analysis of tensegrity structures
- A study for finding the best location of the tensile element along the spiral must be developed.
- A contact mechanic analysis between the robot and the rolling surface is necessary in order to guarantee the turning around a vertical axis and the rolling movement.

CONCLUSIONS

- Due all the geometric variations of the robot are already programed along the rolling movement, the programmer of the robot determines many of the kinematic effects calculated through the equations given in the chapter 2.
- The approximation of the trajectory using a clothoidal fitting is not at all reliable due it requires an improvement of the mathematical process. Also the using of shorter segment will be help to reduce the fitting mistakes found during the analysis.
- The clothoidal fitting could be used to set equations which fit the displacement of the center of the robot.
- Due to the requirements of radial large deformation and almost inexistent longitudinal and tangential deformation, a highly anisotropic material must be chosen for the robot manufacturing. The material found for this purposes could be, with highly certainty, a composed material.
- Curved geometries require an energy analysis in order to find the equilibrium due to the complex load state to which they are subjected.

BIBLIOGRAPHY

[1] J. Y. Zhang, and M. Ohsaki,
2015 "*Tensegrity Structures – Form, Stability, and Symmetry"* Ed. Springer. Tokyo, Japan.

[2] R. E. Skelton, and M. C. De Oliveira,
2009 "*Tensegrity Systems"* Ed. Springer. New York, USA.

[3] Wörnle, Christoph.
2016 "*Mehrkörpersysteme"* .Ed. Springer. Berlin, Germany.

[4] Blach, Checa and Marín
2013 "*Una aproximación a la curva de transición clotoide vista desde Mathematica"* Instituto Universitario de Matemática plicada. Piura, Peru.

[5] R. Wilson
1996 "*Introduction to Graph Theory"* Ed. Longman Group. Essex, England.

[6] K. Ruohonen
2013 "*Graph Theory"* University of British Columbia. Vancouver, Canada.

[7] S. Gast
2017 "*Modellierung von Tensegrity-Strukturen als Mehrkörpersystem und Simulation des dynamischen Verhaltens" Masterarbeit,* Technische Universität Ilmenau. Ilmenau, Germany.

[8] V. Böhm, T. Kaufhold, F. Schale, and K. Zimmermann
2016 "*Spherical Mobile Robot Based on a Tensegrity Structure with Curved Compressed Members"* IEEE International Conference on Advanced Intelligent Mechatronics*,* Alberta, Canada.

[9] V. Böhm and K. Zimmermann
2013 "*Vibration-Driven Mobile Robots Based on Single Actuated Tensegrity Structures"* IEEE International Conference on Robotics and Automation*,* Karlsruhe, Germany.

[10] V. Böhm, T. Kaufhold, S. Sumi, and K. Zimmermann
2017 "*Compliant multistable tensegrity structures"* Mechanism and Machine Theory, Volume 115, Pag 130 – 148, Elsevier.

[11] V. Böhm, I.Zeidis, and K. Zimmermann
2015 "*An approach to the dynamics and control of a planar tensegrity structure with application in locomotion systems"* International Journal of Dynamics and Control, Volume 3, Pag 41 – 49, Springer Verlag, Heildelberg, Germany.

[12] V. Böhm, T. Kaufhold, I.Zeidis, and K. Zimmermann
2017 "*Dynamic analysis of a spherical mobile robot based on a tensegrity structure with two curved compressed members"* Archive of Applied Mechanics, Volume 87, Pag 853 – 864, Springer Verlag, Heildelberg, Germany.

[13] S. Sumi, V. Böhm, and K. Zimmermann
2017 "*A multistable tensegrity structure with a gripper application"* Mechanism and Machine Theory, Volume 114, Pag 204 – 217, Elsevier.

[14] Schramm, Hiller and Bardini.
2014 "*Vehicle Dynamics"* .Ed. Springer – Verlag. Berlin, Germany.

[15] W. Müller and F. Ferber.
2008 "*Technische Mechanik für Ingenieure"* .3th Edition, Ed. Carl Hanser. Leipzig, Germany.

[16] D. Askeland, P. Fulay and W. Wright.
2011 "*The Science and Engineering of Materials"* .6th Edition, Cengage Learning, Stamford, USA.

[17] J. Rodriguez.
2018 "Dinámica*"* Material de Enseñanza, Área de Diseño, Sección Ing. Mecánica, Pontificia Universidad Católica del Perú, Lima, Perú.

[18] J. Rodriguez.
2018 "Resistencia de Materiales 2*"* Material de Enseñanza, Área de Diseño, Sección Ing. Mecánica, Pontificia Universidad Católica del Perú, Lima, Perú.

[19] J. Acosta.
2013 "Ingeniería de Materiales 2*"* Material de Enseñanza, Área de Materiales, Sección Ing. Mecánica, Pontificia Universidad Católica del Perú, Lima, Perú.

[20] E. Carrillo.
2016 "Análisis de cargas en un Bogie Remolcado*"* Tesis de licenciatura en Ingeniería Mecánica, Pontificia Universidad Católica del Perú, Lima, Perú.

[21] P. Moon and D. Spencer.
1971 "*Field theory handbook: Incl. coordinate systems, differential equations and their solutions"* 2nd ed., Springer, Berlin.